Impact of extruder die temperature and nitrogen gas injection on the physical quality of soybean protein meat analogues

By

Neeraj Ghanghas

A thesis submitted to the Faculty of Graduate Studies of

The University of Manitoba

in partial fulfilment of the requirements of the degree of

MASTER OF SCIENCE

Department of Food and Human Nutritional Sciences

University of Manitoba

Winnipeg

Abstract

The food sector is a major contributor to greenhouse gas emissions, and there is an urgent need to shift low-carbon footprint foods. Incorporating plant-based foods, such as meat analogues, in our diets can help mitigate the environmental impact of animal-based foods. Plant-based meat analogues are most commonly produced using high-moisture extrusion cooking, which transforms plant proteins (e.g., soy protein) into products that resemble the sensory characteristics of meat products. However, developing meat analogues with textural attributes similar to meat products is challenging due to the narrow operating range of extrusion process parameters that can provide texturized products with the desired layered and fibrous structure. This study used a novel gas-assisted high-moisture extrusion technique to explore the potential of this technique to improve the textural quality of soy protein-based meat analogues. The degree of texturization as well as the physical quality of meat analogues were studied as a function of long cooling die temperature (DT) and nitrogen gas injection pressure (GP). All extrusion operating parameters were kept constant except for DT (35, 50 and 65 °C) and GP (0, 1 and 2.5 bar). The texture analysis showed that different combinations of DT-GP led to a wide variation in the transversal cutting force (3.97-5.79 N), longitudinal cutting force (3.73-6.00 N), hardness (143.63-194.27 N), chewiness (106.01-150.49 N) and gumminess (115.15-161.85 N). The lowest density was observed for the meat analogues produced at the treatment combination of lowest DT and highest GP. The X-ray microtomography analyses of bubbles formed in the meat analogues produced at a pressure of 2.5 bar GP revealed that variation in DT impacted the properties of the gas volume fraction in the meat analogues. It was observed that an increase in DT led to an increased maximum structure thickness and sphericity while causing a decrease in the major diameter of the bubbles. These wide variations

in textural and microstructural attributes indicate that gas-assisted high-moisture extrusion holds immense potential to improve the sensory properties of meat analogues.

Acknowledgements

With genuine appreciation and respect, I would like to express my heartfelt gratitude to my esteemed advisor, Dr. Filiz Koksel. Her unwavering support and guidance have been a constant source of enlightenment throughout my M.Sc. journey. I consider myself exceptionally fortunate to have had the privilege of working under Dr. Koksel's mentorship. Dr. Koksel not only granted me the invaluable opportunity to work under her mentorship but also consistently provided encouragement, ensuring I remained focused and motivated. Furthermore, I want to acknowledge and express my sincere appreciation to Dr. Jitendra Paliwal and Dr. Rotimi Aluko for their remarkable contributions as distinguished members of my thesis examining committee. Their expertise and invaluable insights played a pivotal role in elevating the depth and quality of my research. I am also grateful for the valuable resources and support they generously provided throughout my research journey, which significantly enriched the content and scope of my work. I want to acknowledge the NSERC Discovery grants program and the NSERC Create grants program for providing financial support.

In the Department of Food and Human Nutritional Sciences laboratories, Alison Ser, Jerry Jin, and Yang Qui provided me with consistent guidance and support. Their willingness to provide training and technical support and to share their expertise was greatly appreciated. I want to acknowledge the invaluable support and training I received from Dr. Catherine Findlay and Dr. Mohammad Nadimi from the Department of Biosystems Engineering in X-ray microtomography, which greatly enhanced my work. I want to express my gratitude for the invaluable administrative assistance provided by the Department of Food and Human Nutritional Sciences support staff, namely Emily Gregorchuk, Samantha Berscheid, Carola Lange, and Helena Marak. Their support and kindness were truly appreciated.

My sincere thanks extend to the remarkable members of the Food Pro Lab, including Dr. Reine-Marie Guillermic, Dr. Nasibeh Younessinaki, Irene Rangira, Ravinder Singh, Siwen Luo and Amanjeet Singh. Their guidance and support were professionally enriching and personally uplifting. I want to express my special gratitude to Ravinder and Siwen for their unwavering support throughout my academic journey, as well as the joyful moments and the lasting memories we have created together. I want to express my deep gratitude for the constant support of my dear friends, including Charu, Yogesh, Laxman, Meghna, Malvika, Pulkit, Harmeen, Varun and all other who have been a part of this incredible journey. Your constant friendship and encouragement have been a cherished blessing throughout this remarkable experience.

Finally, I want to express my deepest gratitude to my beloved family. To my father, Ram Kumar Ghanghas, my mother, Vimla Ghanghas, and my cherished sisters, Sanju and Kiran, as well as all the members of this close-knit family, your boundless love, steady support, and the sacrifices you have made have formed the bedrock of my journey. Your enduring presence and firm belief in me have made all the difference, filling my heart with immeasurable gratitude and love.

Dedication

Dedicated to my beloved parents,

Vimla Ghanghas and Ram Kumar Ghanghas,

For their enduring love, unwavering support, and countless sacrifices.

Table of Contents

List of Tables

List of Figures

List of Abbreviations

ANOVA – Analysis of variance

DT – Long cooling die temperature

F_L – Longitudinal cutting force

F_T – Transversal cutting force

GP – Nitrogen gas injection pressure

SME – Specific mechanical energy

SP – Soy protein blend

TPA – Texture profile analysis

2D – Two dimensional

3D – Three dimensional

$\emptyset$ – Gas volume fraction

ρ – Density

X – Mass fraction

Chapter I: Introduction

The world population is growing rapidly, leading to an increase in the demand for nutritious and healthy foods and posing a severe threat to the environment. Agriculture is one of the main drivers of environmental degradation and is considered responsible for about one-third of the global greenhouse gas (GHG) emissions (Chen et al., 2020; Smetana et al., 2015). In the context of GHG, animal-based foods, commonly consumed worldwide as protein-rich foods, are significant contributors to the agriculture industry. The overall environmental footprint of meat products is almost double that of plant-based foods (Smetana et al., 2015). In addition to their negative environmental impact, animal-based foods are associated with various social, economic and religious concerns.

Meat analogues are products that are made from alternative proteins such as plant proteins, mycoproteins and insect proteins. These products are desired to possess textural quality, visual appearance and taste similar to meat products (GFI, 2020). The availability, cost, techno-functional and nutritional properties of protein ingredients are key factors that decide their application in food formulation, including meat analogues. Soybeans are an excellent source of plant proteins; they contain approximately 40% protein on a dry basis (Medic et al., 2014). Soy protein has a strong presence around the globe, and it is a popular ingredient for meat analogue applications due to its favourable techno-functional properties and nutritional benefits (Vatansever et al., 2020). Soy protein contains a balanced amino acid profile and has a Protein Digestibility Corrected Amino Acid Score (PDCAAS) of 1, comparable to milk protein (Hertzler et al., 2020). Soy protein mainly contains the globulin protein fraction (7S and 11S globulins), which provides it with unique techno-functional properties such as high gelling ability. The 11S globulins possess disulphide

bonds and sulfhydryl groups, which contribute to forming a strong gel network when undergoing a thermo-mechanical process such as extrusion cooking (Liu et al., 2022; Lyu et al., 2022).

High-moisture extrusion cooking is a commonly used technology for industrial-scale meat analogue production because it is an efficient continuous process with high throughput (Cornet et al., 2022; Zhang et al., 2022). Production of plant-based meat analogues requires protein-rich ingredients, high-moisture content (usually > 50% on a wet basis), and a long cooling die attached to the extruder barrel (Caporgno et al., 2020). The process begins with feeding protein ingredients (directly or through a pre-conditioner) and water to the extruder barrel. The continuous rotation of the screws provides mixing and hydration of ingredients. The extruder barrel consists of multiple heating zones, which can be set at desired temperatures to provide thermal energy to the ingredients. As the ingredients flow along the barrel, they experience high heat, pressure and shear, which causes protein denaturation, unfolding, cross-linking and aggregation, forming a molten state known as 'melt' (Cornet et al., 2022). The melt formation facilitates the mobilization, cross-linking, and aggregation of polypeptide chains, and these changes help to form of the characteristic fibrous structure of meat analogues (Samard et al., 2019; Wittek et al., 2021; Zhang et al., 2019). Formation and solidification of the fibrous structure occur in the long cooling die, mainly due to the temperature gradient between the melt and the cooling die (generally < 80 °C). The temperature of the cooling die plays a critical role in this process as it influences the melt's flow profile and rheological properties, affecting the degree of texturization of meat analogues (Cornet et al., 2022; Wittek et al., 2021).

The degree of texturization and the textural quality, such as hardness and chewiness, of meat analogues are very important as meat analogues must mimic the characteristic textural quality of meat products. However, developing meat analogues that mimic the textural quality of meat

products is very challenging because of the complex relationship between extrusion process parameters, and the narrow operating range of those process parameters that provide a desired textural quality. Some of these challenges can be addressed using gas-assisted extrusion cooking based on its success in production of puffed snacks and breakfast cereals (Chan et al., 2019; Luo & Koksel, 2023). Gas-assisted extrusion cooking has been used for manufacturing puffed snacks and breakfast cereals to improve the texture and to obtain a homogeneous porous structure by providing more bubble nucleation sites (Koksel & Masatcioglu, 2018; Sauceau et al., 2011). During extrusion cooking, gases such as nitrogen and carbon dioxide can be injected into an extruder barrel using a gas injection assembly (Chan et al., 2019; Koksel & Masatcioglu, 2018; Luo et al., 2020). Gas injection-assisted high-moisture extrusion cooking can be a novel tool to improve the textural quality of meat analogues by creating microbubbles in the melt. However, the effect of gas-assisted high-moisture extrusion cooking has not been studied so far.

We hypothesized that cooling die temperature and nitrogen gas injection during extrusion dictate how the three-dimensional structure of extrudates develops during extrusion and, in turn, affects the physical quality (density, microstructure, and texture) of meat analogues. Therefore, the primary objectives were set to explore the potential of nitrogen gas injection and manipulation of cooling die temperature to improve the textural (longitudinal and transversal cutting force, degree of texturization and texture profile analysis) and microstructural (density, major bubble diameter, sphericity and structure thickness of bubbles) quality of meat analogues.

References

Caporgno, M. P., Böcker, L., Müssner, C., Stirnemann, E., Haberkorn, I., Adelmann, H., Handschin, S., Windhab, E. J., & Mathys, A. (2020). Extruded meat analogues based on yellow, heterotrophically cultivated Auxenochlorella protothecoides microalgae. *Innovative Food Science & Emerging Technologies*, *59*, 102275. https://doi.org/10.1016/j.ifset.2019.102275

Chan, E., Masatcioglu, T. M., & Koksel, F. (2019). Effects of different blowing agents on physical properties of extruded puffed snacks made from yellow pea and red lentil flours. *Journal of Food Process Engineering*, *42*(3), e12989. https://doi.org/10.1111/JFPE.12989

Chen, C., Chaudhary, A., & Mathys, A. (2020). Nutritional and environmental losses embedded in global food waste. *Resources, Conservation and Recycling*, *160*, 104912. https://doi.org/10.1016/j.resconrec.2020.104912

Cornet, S., Snel, S. J. E., Schreuders, F. K. G., van der Sman, R. G. M., Beyrer, M., & van der Goot, A. J. (2022). Thermo-mechanical processing of plant proteins using shear cell and high-moisture extrusion cooking. *Critical Reviews in Food Science and Nutrition*, *62*(12), 3264–3280. https://doi.org/10.1080/10408398.2020.1864618

GFI. (2020). *Plant-Based Meat, Eggs, and Dairy*. https://gfi.org/wp-content/uploads/2021/01/INN-PBMED-SOTIR-2020-0507.pdf

Hertzler, S. R., Lieblein-Boff, J. C., Weiler, M., & Allgeier, C. (2020). Plant Proteins: Assessing Their Nutritional Quality and Effects on Health and Physical Function. *Nutrients*, *12*(12), 3704. https://doi.org/10.3390/nu12123704

Koksel, F., & Masatcioglu, M. T. (2018). Physical properties of puffed yellow pea snacks produced by nitrogen gas assisted extrusion cooking. *LWT*, *93*, 592–598. https://doi.org/10.1016/J.LWT.2018.04.011

Liu, Y., Huang, Z., Hu, Z., Yu, Z., & An, H. (2022). Texture and rehydration properties of texturised soy protein: analysis based on soybean 7S and 11S proteins. *International Journal of Food Science & Technology*. https://doi.org/10.1111/ijfs.15787

Luo, S., Chan, E., Masatcioglu, M. T., Erkinbaev, C., Paliwal, J., & Koksel, F. (2020). Effects of extrusion conditions and nitrogen injection on physical, mechanical, and microstructural properties of red lentil puffed snacks. *Food and Bioproducts Processing*, *121*, 143–153. https://doi.org/10.1016/J.FBP.2020.02.002

Luo, S., & Koksel, F. (2023). Application of physical blowing agents in extrusion cooking of protein enriched snacks: Effects on product expansion, microstructure, and texture. *Trends in Food Science & Technology*, *133*, 49–64. https://doi.org/10.1016/j.tifs.2023.01.012

Lyu, B., Li, J., Meng, X., Fu, H., Wang, W., Ji, L., Wang, Y., Guo, Z., & Yu, H. (2022). The Protein Composition Changed the Quality Characteristics of Plant-Based Meat Analogues Produced by a Single-Screw Extruder: Four Main Soybean Varieties in China as Representatives. *Foods*, *11*(8), 1112. https://doi.org/10.3390/foods11081112

Medic, J., Atkinson, C., & Hurburgh, C. R. (2014). Current Knowledge in Soybean Composition. *Journal of the American Oil Chemists' Society*, *91*(3), 363–384. https://doi.org/10.1007/s11746-013-2407-9

Samard, S., Gu, B. Y., & Ryu, G. H. (2019). Effects of extrusion types, screw speed and addition of wheat gluten on physicochemical characteristics and cooking stability of meat

analogues. *Journal of the Science of Food and Agriculture*, *99*(11), 4922–4931. https://onlinelibrary.wiley.com/doi/abs/10.1002/jsfa.9722

Sauceau, M., Fages, J., Common, A., Nikitine, C., & Rodier, E. (2011). New challenges in polymer foaming: A review of extrusion processes assisted by supercritical carbon dioxide. *Progress in Polymer Science*, *36*(6), 749–766. https://doi.org/10.1016/j.progpolymsci.2010.12.004

Smetana, S., Mathys, A., Knoch, A., & Heinz, V. (2015). Meat alternatives: life cycle assessment of most known meat substitutes. *The International Journal of Life Cycle Assessment*, *20*(9), 1254–1267. https://doi.org/10.1007/s11367-015-0931-6

Vatansever, S., Tulbek, M. C., & Riaz, M. N. (2020). Low- and High-Moisture Extrusion of Pulse Proteins as Plant-Based Meat Ingredients: A Review. *Cereal Foods World*, *65*(4). https://doi.org/10.1094/CFW-65-4-0038

Wittek, P., Ellwanger, F., Karbstein, H. P., & Emin, M. A. (2021). Morphology Development and Flow Characteristics during High Moisture Extrusion of a Plant-Based Meat Analogue. *Foods*, *10*(8), 1753. https://doi.org/10.3390/foods10081753

Zhang, J., Chen, Q., Kaplan, D. L., & Wang, Q. (2022). High-moisture extruded protein fiber formation toward plant-based meat substitutes applications: Science, technology, and prospect. *Trends in Food Science & Technology*, *128*, 202–216. https://doi.org/10.1016/j.tifs.2022.08.008

Zhang, J., Liu, L., Liu, H., Yoon, A., Rizvi, S. S. H. H., & Wang, Q. (2019). Changes in conformation and quality of vegetable protein during texturization process by extrusion. *Critical*

Reviews in Food Science and Nutrition, *59*(20), 3267–3280. https://doi.org/10.1080/10408398.2018.1487383

Chapter II: Literature Review

2.1. Extrusion cooking, a versatile food processing technique

Extrusion is a technique that utilizes a combination of unit operations such as mixing, conveying, heating, shearing, shaping, and cutting (Fellows, 2017; Morales Alvarez, 2020). The applications of extrusion technology can be found in different fields, such as foods, plastic, metal fabrication, and ceramics (Li, 2021; Wittek & Emin, 2017). The use of extrusion technology in the food industry dates back to the late 1930s for the continuous production of pasta; which is a cold extrusion process that involves temperatures below 100 °C (Bouvier & Campanella, 2014a; Fellows, 2017; Riaz, 2000). The cooking extrusion (hot extrusion) process was developed in the late 1940s to produce animal feed. The use of extrusion cooking to produce foods for human consumption started in the 1960s. Ready-to-eat breakfast cereals were the first foods made using a cooking extruder (Judson Harper, 2019). In the last six decades, many advancements have been made in extrusion technology to process various agri-food-based raw materials. Nowadays, extrusion cooking is commonly used in the agri-food processing sector to produce a wide variety of products, such as breakfast cereals, puffed snacks, low moisture texturized vegetable proteins and high-moisture meat analogues (Mościcki & van Zuilichem, 2011).

Extrusion cooking is an HTST (high temperature-short time) processing technology with a process temperature of up to 170 °C and a residence time of 2-5 minutes (Cornet et al., 2022; Judson Harper, 2019). A schematic illustration of a twin screw extruder is presented in Figure 2.1. A generic extrusion setup consists of a pre-conditioner and an extruder. A pre-conditioner is an ancillary unit of the extrusion process (Bouvier & Campanella, 2014b). Its primary purpose is to preheat and prehydrate the raw materials (dry ingredients such as flour and proteins). An extruder consists of the following essential components: (i) a motor to rotate the shafts, (ii) a feeder for

storing and feeding raw materials, (iii) a water injection port, (iv) a barrel with multiple temperature zones, (v) a screw assembly encased in the barrel, and (vi) a die.

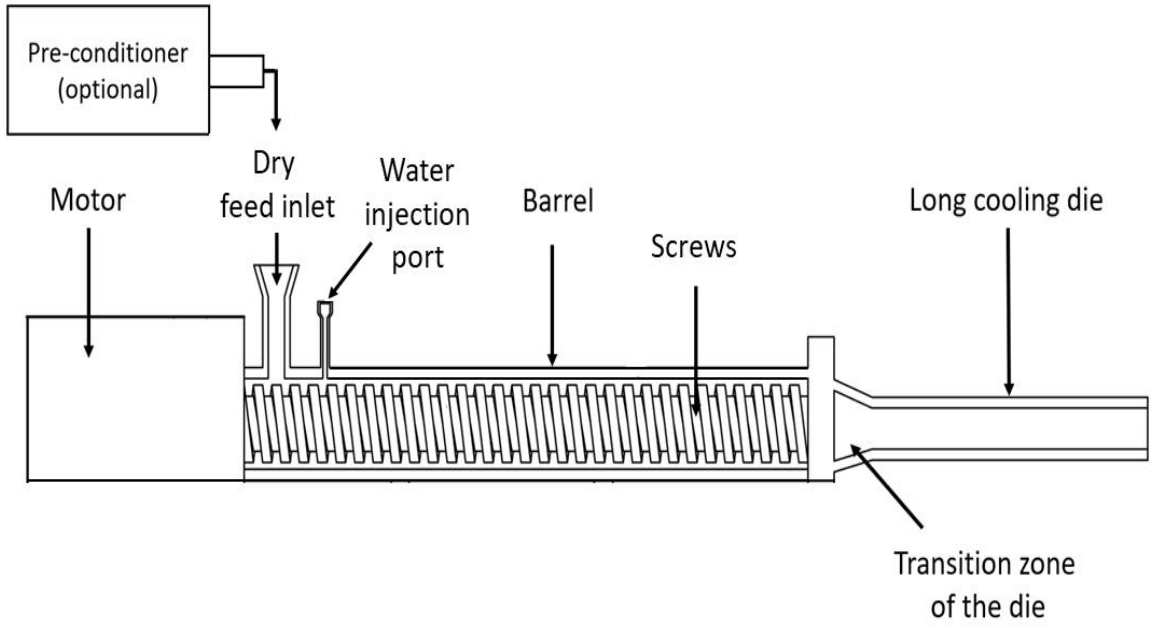

Figure 2.1: Schematic illustration of an extruder with a long cooling die for high-moisture extrusion cooking.

2.2. High-moisture extrusion cooking and protein texturization

2.2.1. High-moisture extrusion cooking for meat analogue production

During extrusion, raw materials are cooked under severe conditions (high temperature, shear, and pressure), and they undergo complex changes such as denaturation or aggregation of proteins, depolymerization of starch, and expansion and solidification of food structure when exiting the die (Bouvier & Campanella, 2014b; Fellows, 2017). A general extrusion cooking

process starts with feeding raw materials (dry ingredients and water) into the barrel. The dry ingredients are fed into the barrel using a (volumetric or gravimetric) feeder. At the same time, water is pumped into the barrel through the water injection port. In the barrel section, the raw materials are mixed, hydrated and transformed into a molten mass known as 'melt'. Finally, the melt is shaped in the die, attached at the end of the barrel section, in the form of extrudates (Bouvier & Campanella, 2014b). For high-moisture extrusion cooking during meat analogue production, the die used is a long cooling die where texturization of the melt occurs that forms the characteristic layered/fibrous structure of extrudates that resemble animal meat.

Extrusion processing requirements can vary depending on the desired final product (e.g., meat analogues vs breakfast cereals). Those extrusion requirements include but not limited to types of raw materials, extrusion variables such as dry and wet feed rates, barrel temperature profile, and screw speed and configuration, and the type of die.

For meat analogue production, high-moisture extrusion cooking is widely used on an industrial scale. The primary requirements for high-moisture extrusion cooking are a blend of protein-rich ingredients, a moisture content above 50% (w.b.), which can be supplied partially through a pre-conditioner or directly injected into the extruder barrel, and a long cooling die at the end of the extruder barrel (Beniwal et al., 2021a; Cornet et al., 2022; Vatansever et al., 2020a; Wittek et al., 2021). Depending on the desired characteristics of the final meat analogue, the processing conditions for the barrel (temperature profile, and screw speed and configuration), and die (die length and cooling rate) sections can be altered (Pietsch et al., 2017).

According to Cornet et al. (2022), high-moisture extrusion cooking is comprised of three stages: mixing and hydration, thermomechanical processing/melting, and cooling. In the first stage of extrusion, when the protein-rich ingredients are hydrated and heated, protein starts to unfold

and its solubility increases. These changes depend considerably on the conformation and structure of the proteins present in the raw material (Wild, 2016). As proteins are conveyed towards the die end of the extruder, the cumulative thermo-mechanical stresses they endure increase, which facilitate further unfolding of the protein structure (Arora et al., 2020), making the reactive groups of amino acids more accessible to new interactions (Wild, 2016). In order to determine the extent of changes that proteins undergo during high-moisture extrusion cooking, protein solubility studies have been commonly carried out (Immonen et al., 2021; Lee et al., 2022; Osen et al., 2015; Pietsch et al., 2019; Samard et al., 2019; Wittek et al., 2021; Zhang et al., 2022). Most of these studies have reported that both non-covalent (hydrogen bonds and electrostatic and hydrophobic interactions), and covalent (disulfide bonds) interactions are involved in forming fibrous structures. However, protein solubility analyses of extrudates made from different protein sources or using different extrusion conditions reported in various studies lack agreement on the types of bonds and interactions that play critical roles in structure formation (Chen et al., 2011; Chiang et al., 2019; Osen et al., 2015; Pietsch et al., 2017, 2019; Wittek et al., 2021). These inconsistencies can stem from the differences in protein fractions (such as the percentage of globulin fractions present in the total protein) in the protein-rich raw material (e.g., soy vs. pea) and differences in protein composition, structure and techno-functionality due to protein extraction technique used (Karaca & Nickerson, 2022; Yang et al., 2021). For example, the higher degree of protein denaturation during wet protein extraction process can result in strong covalent bonds between proteins that are resistant to any further change during extrusion cooking (Wittek et al., 2021). Although different studies disagree on the effect of high-moisture extrusion cooking of meat analogues on the type of protein-protein interactions involved, it is widely accepted that proteins

first need to be brought to a continuous molten matrix (melt) in the extruder barrel (Cornet et al., 2022; Ryu, 2020).

In the second stage of high-moisture extrusion cooking, the raw materials are transformed into a melt due to thermomechanical processing. Sandoval et al. (2019) proposed that the melt is a homogeneous single-phase system that undergoes phase separation upon cooling in the cooling die. This phase separation results in a multi-phase system in the cooling die that contains protein-rich and water-rich domains. This hypothesis conflicts with the more recent studies that a multi-phase system is already present in the screw section of the extruder barrel in addition to being present along the length of the cooling die (Chen et al., 2022; Wittek et al., 2021, 2021). Regardless of where this multi-phase system first appears, the melt developed during thermo-mechanical processing underlays the anisotropic fibrous structure of the end product.

According to Wittek, Ellwanger, et al. (2021), the multi-phase melt system starts to form as soon as the melting of protein begins. The melting of proteins permits the mobility of protein molecules and promotes more interactions between the denatured protein molecules that lead to the formation of protein fractions that are immiscible in each other, causing phase separation in the melt (Grinberg & Tolstoguzov, 1997; Tolstoguzov, 1993; Wittek et al., 2021). The protein phase separation in the melt can cause water redistribution between these protein fractions leading to the formation of water-rich and water-poor domains (Wittek et al., 2021). This water redistribution predominantly depends on the nature of protein ingredients (e.g., their composition and structure). According to Wittek, Karbstein, et al. (2021) and Wittek, Zeiler, et al. (2021) the hydrophilic and hydrophobic character of proteins during thermo-mechanical processing is a driving factor that influences water redistribution in the melt; due to differences in protein solubility in water, they tend to phase separate.

The third stage of high-moisture extrusion cooking is cooling of melt using a long cooling die (illustrated in Figure 2.1) attached to the extruder barrel. Generally, a long cooling die consists of (i) a tapered, uncooled transition zone and (ii) a long and cooled section. Transformation of the melt into a layered and/or fibrous structure of meat analogues that resemble animal meat is finalized in the long cooling die and depends on the melt and die temperature.

2.2.2. Importance of cooling die temperature during high-moisture extrusion cooking

The temperature of the melt entering the die plays a crucial role in forming the anisotropic fibrous structure. It was reported by Wittek, Ellwanger, et al. (2021) that higher melt temperatures (e.g., 125 °C) produce a better fibrous structure than at lower temperatures (e.g., 95 °C) for soy protein texturization. Understanding the mechanism of fibrous structure formation requires information about the changes in flow characteristics of the melt when it enters the transition zone and as it flows through the long and cooled section of the die. The change in flow characteristics of the melt starts in the uncooled transition zone and continues in the long and cooled section (as illustrated in Figure 2.2) due to the change in geometrical dimensions and higher temperature gradient between the melt and the die wall in the long and cooled section of the die (Sandoval et al., 2019; Wittek et al., 2021).

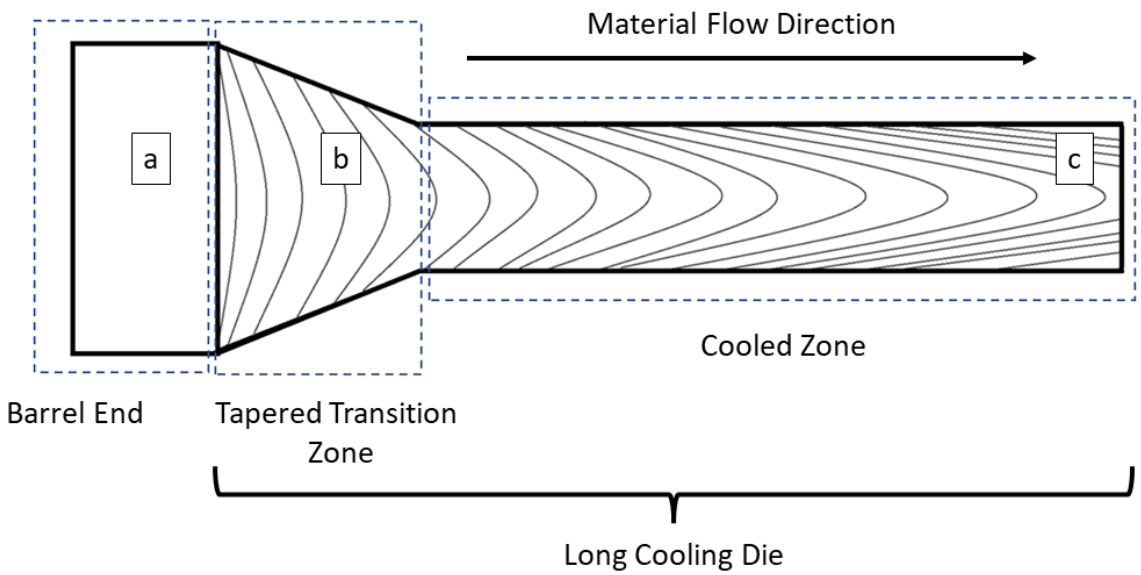

Figure 2.2: Velocity profile of melt in the long cooling die, adapted from Wittek, Ellwanger, et al. (2021).

At the beginning of the transition zone, the melt has flat flow profile, i.e., the water-rich and water poor phases of the melt is oriented perpendicular to the flow direction (Figure 2.2a), but it starts to develop a parabolic flow profile (Figure 2.2b) as it flows towards the entrance of the cooled section of the die. The change in the flow profile continues in the cooling section and becomes more pointed (Figure 2.2c) as it flows towards the exit of the die. This change is caused by the increase in melt viscosity, which primarily depends on the cooling die temperature. The viscosity is lowest at the hot core of the melt and highest at the walls of the die. This viscosity gradient across the cross-section of the melt affects the melt's velocity profile by deaccelerating the melt closer to the walls of the die and making the flow profile more elongated. The dispersed and continuous phases of the melt elongate and solidify as the melt flows along the long cooling die, leading to the formation of a fibrous structure in meat analogue (Wittek et al., 2021, 2021).

Thus, cooling die temperature is one of the crucial high-moisture extrusion cooking parameters that dictates the fibrous structure formation of the meat analogues.

2.2.3. Texturization of soy protein to make meat analogues using high-moisture extrusion cooking

2.2.3.1. Soy protein

East and South-East Asian cuisines rely on soybeans. Traditional soybean products including natto, tofu, miso, and shoyu, are still consumed in these regions and expanding worldwide. Even though Asian countries have a long history of soybean cultivation and use, Brazil, USA, and Argentina now contribute to 81% of global soybean production (Matsumura et al., 2017). In Canada, the soybean production was 6.2 Mt in the crop year 2021-22 and is forecasted to be 6.5 Mt in 2022-23 (Flint & McDougall, 2023). The production of soybean is rapidly increasing because of the economic value of end products such as oils and proteins (Assefa et al., 2018). The approximate amount of fat, protein, carbohydrate, and ash in soybean seed is 18-20%, 40-45%, 25-35%, and 3%, respectively (Swain et al., 2004). It is also considered a rich source of micronutrients such as calcium, iron, magnesium, phosphate, zinc, and vitamin B (Prak, 2006). Soybeans are commercially processed to extract oil and protein; the remaining by-products are used as animal feed (Jensen, 2012). Soy protein products are commercially available in the form of defatted soy flour, soy protein concentrates, and soy protein isolates and contain approximately 50-56%, 65-71%, and > 90% protein (on a dry weight basis), respectively (Swain et al., 2004; Webb et al., 2023).

For the production of defatted soy flour, soybeans go through a series of unit operations such as cleaning, dehulling, flaking and defatting by solvent extraction method (Singh, 2021).

Although defatted soy flour has high protein content, it is not a preferred ingredient for food applications because of its beany and grassy flavours (Hansen, 2020). In contrast, soy protein concentrates and isolates are commonly used to produce meat analogues (Lee et al., 2022; Ma et al., 2022). Soy protein concentrates and isolates are produced from the defatted soy flour; this is done by removing soluble and insoluble carbohydrates from the defatted soy flour. The process starts with solubilizing defatted soy flour in an aqueous solution (pH 8-9) to form two fractions/phases. Insoluble carbohydrates remain in the solid phase, while soluble carbohydrates and proteins get solubilized in the aqueous phase (Thrane et al., 2017). The aqueous phase is separated from the solid phase, and the pH of the aqueous phase is reduced to the isoelectric point (pH 4.2-4.5) of the proteins, leading to the precipitation of proteins. The precipitated proteins are separated from the supernatant by centrifugation. The proteins are further neutralized by adjusting the pH and finally dried to obtain protein in powder form (Hansen, 2020; Thrane et al., 2017). Spray drying is a popular method used in the commercial-scale production process of proteins. In addition, to produce food-grade protein isolates, pasteurization of proteins is done before the spray drying stage to meet regulatory requirements (Hansen, 2020; Hansen et al., 2022).

Soy protein is a heterogeneous mixture of globulin protein subunits with a molecular weight of 8-600 kDa (Wolf, 1970). Based on the sedimentation coefficients, these protein subunits can be classified into four different types: 2S, 7S, 11S, and 15S (Tay et al., 2005). The 2S and 15S are minor protein fractions of soybean, accounting for about 15-20% and 11% of total soy protein, respectively. The molecular weight of 2S and 15S subunits range from 8-21.5 kDa and 506-600 kDa, respectively (Al-Bakkush, 2008; Wolf, 1970). The 7S and 11S are the major protein fractions. Together, they contribute about 65% of the total protein and dictate the overall techno-functional properties of soy protein (Rasheed et al., 2020; Vatansever et al., 2020b). The 7S subunit, also

known as β-conglycinin, is approximately 30% of total protein and is a trimeric protein having a molecular weight in the range of 180-210 kDa (Al-Bakkush, 2008; Thrane et al., 2017; Wolf, 1970). Due to the small molecular size and lack of covalent disulfide bonds, β-conglycinin has good emulsification properties (Dagorn-Scaviner et al., 1986; Fukushima, 2004). On the other hand, the 11S subunit, also known as glycinin, is approximately 35% of the total protein and is a heterogenous oligomeric protein with molecular weight in the range of 340-375 kDa (Al-Bakkush, 2008; Wolf, 1970). The glycinin subunit has good gelling properties because of its ability to form disulphide intermolecular crosslinks. These crosslinks contribute to the elasticity and strength of the gel (Hansen et al., 2022; Shand et al., 2007; Wolf, 1970). The ratio of β-conglycinin to glycinin in soy protein can vary between 0.5-1.3 due to varietal differences (Singh, 2021). The ratio of β-conglycinin to glycinin decides the overall techno-functional properties of soy proteins. Soy protein forms stronger heat-induced gels than other legume proteins due to a comparatively higher amount of glycinin than other legumes. Proteins with good gelling properties have a high potential to produce texturized products (Schreuders et al., 2019). Since soy protein forms strong gels, it is preferred for making meat analogues (Schlangen et al., 2023; Schreuders et al., 2019).

2.2.3.2. Effect of extrusion process parameters on soy protein texturization

Though soy protein can form a good texturized product, its texturization highly depends on extrusion cooking parameters. The extrusion parameters are classified into (1) process parameters and (2) system parameters, together which influence the characteristics of the extruded products. The process parameters include raw material feed rate, moisture content, the temperature profile of the barrel, screw speed and configuration, and die temperature. The second group of parameters is system parameters, which depend on the process parameters and include specific mechanical energy, viscosity and temperature of the melt, the residence time of the melt in the

extruder, and die pressure (Maung et al., 2021). The feed moisture content and process temperature are two main parameters that significantly influence the texturization process and extrudate properties.

2.2.3.2.1. Feed moisture content

Feed moisture acts as an energy transfer medium during extrusion cooking, influences melt viscosity and specific mechanical energy input to the melt and participates in chemical reactions during extrusion cooking (Zhang et al., 2018, 2020). As an increase in feed moisture content reduces melt viscosity during high-moisture extrusion cooking (Maung et al., 2021), a higher moisture can directly affect the protein texturization by influencing the flow behaviour of melt in the cooling die as explained in previous sections (Chen et al., 2010; Maung et al., 2021; Zahari et al., 2021; Zhang et al., 2020).

The textural quality attributes of meat analogues, such as hardness, chewiness, cutting strength, etc., depend on their fibrous structure, which can be significantly impacted by the feed moisture level. A meat analogue produced at increased moisture content is usually soft, less chewy, and requires a lower cutting strength. For example, Zahari et al. (2020) reported a decreasing trend in the hardness, and chewiness values of soy based meat analogues with increase in moisture content from 65% to 75%. Moisture level also impacted the longitudinal and transversal cutting strength of meat analogues (Zahari et al., 2021), which is used to analyze the degree of texturization, i.e., the ratio of longitudinal and transversal cutting. The moisture content is inversely related to the cutting strength in longitudinal and transversal directions (Kantanen et al., 2022a; Zahari et al., 2021). Various studies on meat analogues made from vegetable proteins such as soy (Zahari et al., 2020), faba bean (Ferawati et al., 2021; Kantanen et al., 2022a; Saldanha do Carmo et al., 2021), yellow field pea (Ferawati et al., 2021), lupin (Palanisamy et al., 2019), and

pea (Zahari et al., 2021) have reported a similar trend for the values of hardness, chewiness and cutting strength (longitudinal and transversal) with increasing moisture content.

2.2.3.2.2. Temperature

Temperature is another important parameter that impacts texturization of proteins and the characteristic properties of meat analogues. As described in previous sections, to produce texturized protein products, the formation of a melt is crucial (Cornet et al., 2022; Ryu, 2020). The high temperature in the barrel contributes to protein unfolding and increased mobility of protein molecules, facilitating the formation of new bonds that are essential for developing a fibrous texture (Arora et al., 2020; Schmid et al., 2022). Temperature also affects the techno-functional properties of proteins. According to Osen et al. (2014), the techno-functional properties such as solubility and water holding capacity of proteins at temperatures lower than the protein denaturation temperature can be substantially different from those at higher temperatures. They can indirectly affect the specific mechanical energy during extrusion cooking due to changes in the viscosity of the melt.

The barrel temperature affects not only melt formation but also melt viscosity (Chen et al., 2010; Osen et al., 2014) and melt temperature (Wittek, Zeiler, et al., 2021), both of which significantly impact the texturization process in the long cooling die. Wittek, Karbstein, et al. (2021b) reported that an increase in melt temperature from 115 °C to 135 °C resulted in a significant increase in the peak cutting force during texture measurements of the extrudate. The value of the degree of texturization increased from 1 to 1.5, denoting a significant improvement in the fibrous structure (Wittek, Karbstein, et al., 2021b). The barrel temperature profile should be selected considering that it is sufficient to produce melt and mobilize protein molecules but not

too high to cause detrimental effects on extrudates such as the Maillard reaction resulting in dark colour extrudates (Sun et al., 2022).

2.3. Gas-assisted extrusion cooking

Extrusion cooking is a complex food processing technology. The characteristic properties of the extrudates are controlled by the process variables such as feed rate, moisture content, screw speed and profile, and barrel temperature profile (Zahari et al., 2022). The effect of these process variables on final product properties is unknown, and generally, empirical knowledge is used to design novel extruded products (Beniwal et al., 2021b; Schmid et al., 2022). The empirical approach involves controlling the thermomechanical process by manipulating the process variables and establishing a relationship between process variables and the properties (mainly textural properties) of the final product (Emin, 2022).

The textural properties, such as hardness, chewiness, and gumminess, are the most critical sensory attributes of any food product that decide consumer acceptability. The textural quality of extruded food products has been reported to correlate highly with their microstructure (Guillermic et al., 2021). Like other extruded foods, in meat analogues, the processing conditions can affect the microstructure, ultimately affecting their textural characteristics (Kantanen et al., 2022b; Wittek et al., 2021). Although it is will accepted that microstructure can have significant impact the textural properties of meat analogues, the relationship between microstructure and textural properties is very complex and has not been widely studied.

In conventional extrusion cooking, controlling, and predicting the microstructure of extrudates in advance and solely based on extrusion process parameters is very challenging (Rizvi et al., 1995). For example, meat analogues are desired to have good fibrous structure (high degree

of texturization) along with textural attributes (such as hardness, chewiness, and juiciness) like meat products. But designing such products solely based on an empirical approach is sometimes very difficult, time consuming, and resource intensive. Development of meat analogues with desired texture require focus on the microscopic level (Zhong et al., 2023). Designing meat analogues with micro bubbles in its matrix can help to address these challenges. A novel, simple and inexpensive technique, i.e., gas-assisted extrusion cooking, can be used to create micro bubbles in meat analogue matrix. The gas-assisted extrusion has proven to be an effective technique for manipulating the microstructure of low-moisture extruded products to improve their textural qualities (Guillermic et al., 2021; Koksel & Masatcioglu, 2018; Luo & Koksel, 2023).

In gas-assisted extrusion cooking, blowing agents are used to create micro bubbles in food matrix. Blowing agents are classified into physical and chemical blowing agents, depending on their mode of action (Ferdinand et al., 1990, 1992). The chemical blowing agents such as $NaHCO_3$, and citric acid are fed into the extruder along with other feed ingredients and decompose in the barrel leading to gas production. For example, decomposition of sodium bicarbonate in the extruder barrel produces CO_2, which acts as a blowing agent. The disadvantage with the use of chemical blowing agents is that they can cause undesirable changes such as change of melt pH, and darker colour of extrudates (Berrios et al., 2005; Luo & Koksel, 2023; Rokkonen et al., 2021). In contrast, physical blowing agents with low water solubility values, such as nitrogen, are injected into the extruder barrel in gaseous state from a gas cylinder and are mixed with the melt under high temperature, pressure, and shear conditions to create microscopic gas bubbles (Ferdinand et al., 1990; Koksel & Masatcioglu, 2018). It is desired that a blowing agent intended to be used for food extrusion must be inert, affordable, environment-friendly, non-hazardous, and is widely available (Luo & Koksel, 2023; Rezaei et al., 2014). Nitrogen gas is one of the physical blowing

agents that meets all the above mentioned criteria and is a suitable candidate for application in gas-assisted food extrusion cooking (Rezaei et al., 2014).

The gas-assisted high-moisture extrusion cooking requires an additional unit i.e., gas injection assembly, attached to the conventional high-moisture extrusion cooking setup (Figure 2.1). A typical gas-assisted extrusion cooking setup is illustrated in Figure 2.3. The gas injection assembly consists of a pressurized gas tank and a pressure control valve. In this process, a gas such as nitrogen is continuously supplied to the extruder barrel from a pressurized gas tank. The gas injection pressure is regulated with the help of a pressure control valve. Though gas-assisted high-moisture extrusion cooking has not been carried out yet, it is expected that when gas is introduced into the barrel, it will mix and partially or entirely dissolve in the melt (depending on the type of gas), as reported for low moisture extrusion (Luo & Koksel, 2023). The introduction of gas in the melt will cause production of micro bubbles in the melt and it is assumed that as melt flows through the long cooling die there will be a change in the bubble characteristics such as size and shape. As explained earlier, the long cooling die temperature affects the fibrous structure development so it also expected that bubble characteristics will be impacted by the long cooling die temperature.

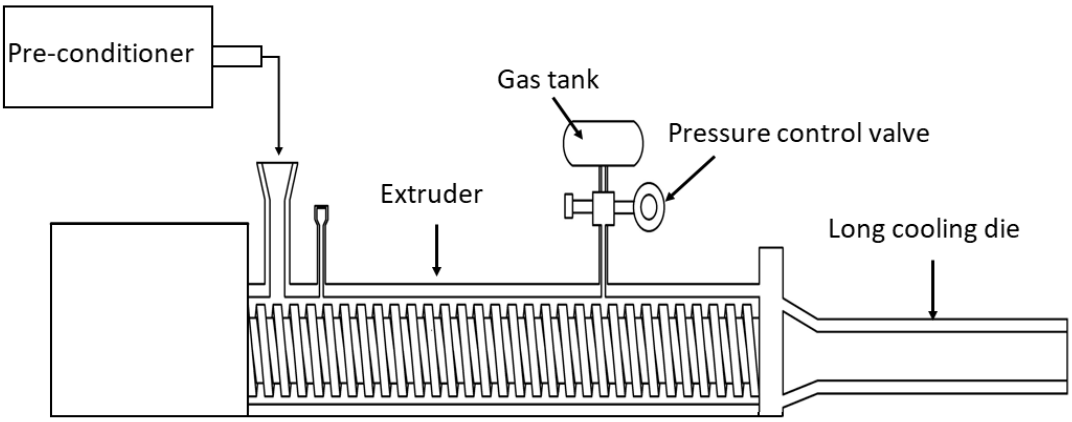

Figure 2.3: Schematic illustration of an high-moisture extrusion cooking setup with a gas injection assembly.

References

Al-Bakkush, A.-A. (2008). *Improvement of functional properties of soy protein* [Heriot-Watt University]. http://hdl.handle.net/10399/2253

Arora, B., Yoon, A., Sriram, M., Singha, P., & Rizvi, S. S. H. (2020). Reactive extrusion: A review of the physicochemical changes in food systems. In *Innovative Food Science and Emerging Technologies* (Vol. 64, p. 102429). Elsevier Ltd. https://doi.org/10.1016/j.ifset.2020.102429

Assefa, Y., Bajjalieh, N., Archontoulis, S., Casteel, S., Davidson, D., Kovács, P., Naeve, S., & Ciampitti, I. A. (2018). Spatial Characterization of Soybean Yield and Quality (Amino Acids, Oil, and Protein) for United States. *Scientific Reports*, *8*(1), 14653. https://doi.org/10.1038/s41598-018-32895-0

Beniwal, A. S., Singh, J., Kaur, L., Hardacre, A., & Singh, H. (2021a). Meat analogs: Protein restructuring during thermomechanical processing. *Comprehensive Reviews in Food Science and Food Safety*, *20*(2), 1221–1249. https://doi.org/10.1111/1541-4337.12721

Beniwal, A. S., Singh, J., Kaur, L., Hardacre, A., & Singh, H. (2021b). Meat analogs: Protein restructuring during thermomechanical processing. *Comprehensive Reviews in Food Science and Food Safety*, *20*(2), 1221–1249. https://doi.org/10.1111/1541-4337.12721

Berrios, J. D. J., Wood, D. F., Whitehand, L., & Pan, J. (2005). Sodium bicarbonate and the microstructure, expansion and color of extruded black beans. *Journal of Food Processing and Preservation*, *28*(5), 321–335. https://doi.org/10.1111/j.1745-4549.2004.24008.x

Bouvier, J., & Campanella, O. H. (2014a). Generic Extrusion Processes. In *Extrusion Processing Technology*. John Wiley & Sons, Ltd. https://doi.org/10.1002/9781118541685.CH1

Bouvier, J., & Campanella, O. H. (2014b). The Generic Extrusion Process III. In *Extrusion Processing Technology* (pp. 243–309). Wiley. https://doi.org/10.1002/9781118541685.ch6

Chen, F. L., Wei, Y. M., & Zhang, B. (2011). Chemical cross-linking and molecular aggregation of soybean protein during extrusion cooking at low and high moisture content. *LWT - Food Science and Technology*, *44*(4), 957–962. https://doi.org/10.1016/J.LWT.2010.12.008

Chen, F. L., Wei, Y. M., Zhang, B., & Ojokoh, A. O. (2010). System parameters and product properties response of soybean protein extruded at wide moisture range. *Journal of Food Engineering*, *96*(2), 208–213. https://doi.org/10.1016/j.jfoodeng.2009.07.014

Chen, Q., Zhang, J., Zhang, Y., Kaplan, D. L., & Wang, Q. (2022). Protein-amylose/amylopectin molecular interactions during high-moisture extruded texturization toward plant-based meat substitutes applications. *Food Hydrocolloids*, *127*, 107559. https://doi.org/10.1016/J.FOODHYD.2022.107559

Chiang, J. H., Loveday, S. M., Hardacre, A. K., & Parker, M. E. (2019). Effects of soy protein to wheat gluten ratio on the physicochemical properties of extruded meat analogues. *Food Structure*, *19*, 100102. https://doi.org/10.1016/J.FOOSTR.2018.11.002

Cornet, S., Snel, S. J. E., Schreuders, F. K. G., van der Sman, R. G. M., Beyrer, M., & van der Goot, A. J. (2022). Thermo-mechanical processing of plant proteins using shear cell and high-moisture extrusion cooking. *Critical Reviews in Food Science and Nutrition*, *62*(12), 3264–3280. https://doi.org/10.1080/10408398.2020.1864618

Dagorn-Scaviner, C., Gueguen, J., & Lefebvre, J. (1986). A comparison of interfacial behaviours of pea (Pisum sativum L.) legumin and vicilin at air/water interface. *Food / Nahrung*, *30*(3–4), 337–347. https://doi.org/10.1002/food.19860300332

Emin, M. A. (2022). Key technological advances of extrusion processing. In P. Juliano, K. Knoerzer, J. Sellahewa, M. H. Nguyen, & R. Buckow (Eds.), *Food Engineering Innovations Across the Food Supply Chain* (1st ed., pp. 131–148). Elsevier. https://doi.org/10.1016/B978-0-12-821292-9.00005-4

Fellows, P. J. (2017). Extrusion Cooking. In *Food Processing Technology - Principles and Practice (4th Edition)*. Elsevier. https://app.knovel.com/hotlink/khtml/id:kt0114838H/food-processing-technology/extrusion-cooking

Ferawati, F., Zahari, I., Barman, M., Hefni, M., Ahlström, C., Witthöft, C., & Östbring, K. (2021). High-Moisture Meat Analogues Produced from Yellow Pea and Faba Bean Protein Isolates/Concentrate: Effect of Raw Material Composition and Extrusion Parameters on Texture Properties. *Foods 2021, Vol. 10, Page 843*, *10*(4), 843. https://doi.org/10.3390/FOODS10040843

Ferdinand, J. M., Clark, S. A., & Smith, A. C. (1992). Structure formation in extrusion-cooked starch-sucrose mixtures by carbon dioxide injection. *Journal of Food Engineering*, *16*(4), 283–291. https://doi.org/10.1016/0260-8774(92)90004-P

Ferdinand, J. M., Lai-Fook, R. A., Ollett, A.-L., Smith, A. C., & Clark, S. A. (1990). Structure formation by carbon dioxide injection in extrusion cooking. *Journal of Food Engineering*, *11*(3), 209–224. https://doi.org/10.1016/0260-8774(90)90028-7

Flint, J., & McDougall, T. (2023). *Canada: Outlook for principal field crops*. https://agriculture.canada.ca/en/sector/crops/reports-statistics/canada-outlook-principal-field-crops-2023-03-21

Fukushima, D. (2004). Soy proteins. In *Proteins in Food Processing* (pp. 123–145). Elsevier. https://doi.org/10.1533/9781855738379.1.123

Grinberg, V. Y., & Tolstoguzov, V. B. (1997). Thermodynamic incompatibility of proteins and polysaccharides in solutions. *Food Hydrocolloids*, *11*(2), 145–158. https://doi.org/10.1016/S0268-005X(97)80022-7

Guillermic, R.-M., Aksoy, E. C., Aritan, S., Erkinbaev, C., Paliwal, J., & Koksel, F. (2021). X-Ray microtomography imaging of red lentil puffed snacks: Processing conditions, microstructure and texture. *Food Research International*, *140*, 109996. https://doi.org/10.1016/j.foodres.2020.109996

Hansen, L. (2020). *The optimization and scale-up of protein extraction and impact on struictural and functional properties* [University of Minnesota]. https://hdl.handle.net/11299/216768

Hansen, L., Bu, F., & Ismail, B. P. (2022). Structure-Function Guided Extraction and Scale-Up of Pea Protein Isolate Production. *Foods*, *11*(23), 3773. https://doi.org/10.3390/foods11233773

Immonen, M., Chandrakusuma, A., Sibakov, J., Poikelispää, M., & Sontag-Strohm, T. (2021). Texturization of a Blend of Pea and Destarched Oat Protein Using High-Moisture Extrusion. *Foods*, *10*(7), 1517. https://doi.org/10.3390/foods10071517

Jensen, A. M. (2012). *Development and characterization of high performance solvent cast soy protein isolate composite films* [University of Guelph]. http://hdl.handle.net/10214/3681

Judson Harper, A. M. (2019). *Extrusion Of Foods*. https://doi.org/10.1201/9780429290428

Kantanen, K., Oksanen, A., Edelmann, M., Suhonen, H., Sontag-Strohm, T., Piironen, V., Ramos Diaz, J. M., & Jouppila, K. (2022a). Physical Properties of Extrudates with Fibrous

Structures Made of Faba Bean Protein Ingredients Using High Moisture Extrusion. *Foods*, *11*(9), 1280. https://doi.org/10.3390/foods11091280

Kantanen, K., Oksanen, A., Edelmann, M., Suhonen, H., Sontag-Strohm, T., Piironen, V., Ramos Diaz, J. M., & Jouppila, K. (2022b). Physical Properties of Extrudates with Fibrous Structures Made of Faba Bean Protein Ingredients Using High Moisture Extrusion. *Foods*, *11*(9), 1280. https://doi.org/10.3390/foods11091280

Karaca, A. C., & Nickerson, M. T. (2022). Developing Value-Added Protein Ingredients from Wastes and Byproducts of Pulses: Challenges and Opportunities. *ACS Omega*, *7*(22), 18192–18196. https://doi.org/10.1021/ACSOMEGA.2C00414

Koksel, F., & Masatcioglu, M. T. (2018). Physical properties of puffed yellow pea snacks produced by nitrogen gas assisted extrusion cooking. *LWT*, *93*, 592–598. https://doi.org/10.1016/j.lwt.2018.04.011

Lee, J. S., Oh, H., Choi, I., Yoon, C. S., & Han, J. (2022). Physico-chemical characteristics of rice protein-based novel textured vegetable proteins as meat analogues produced by low-moisture extrusion cooking technology. *LWT*, *157*, 113056. https://doi.org/10.1016/J.LWT.2021.113056

Lee, J.-S., Choi, I., & Han, J. (2022). Construction of rice protein-based meat analogues by extruding process: Effect of substitution of soy protein with rice protein on dynamic energy, appearance, physicochemical, and textural properties of meat analogues. *Food Research International*, *161*, 111840. https://doi.org/10.1016/j.foodres.2022.111840

Li, X. (2021). *Effects of extrusion cooking on physical and nutritional quality of puffed snacks made from blends of barley and green lentil flours*. https://mspace.lib.umanitoba.ca/xmlui/handle/1993/35752

Luo, S., & Koksel, F. (2023). Application of physical blowing agents in extrusion cooking of protein enriched snacks: Effects on product expansion, microstructure, and texture. *Trends in Food Science & Technology*, *133*, 49–64. https://doi.org/10.1016/j.tifs.2023.01.012

Ma, K. K., Grossmann, L., Nolden, A. A., McClements, D. J., & Kinchla, A. J. (2022). Functional and physical properties of commercial pulse proteins compared to soy derived protein. *Future Foods*, *6*, 100155. https://doi.org/10.1016/j.fufo.2022.100155

Matsumura, Y., Sirison, J., Ishi, T., & Matsumiya, K. (2017). Soybean lipophilic proteins — Origin and functional properties as affected by interaction with storage proteins. *Current Opinion in Colloid & Interface Science*, *28*, 120–128. https://doi.org/10.1016/j.cocis.2017.04.004

Maung, T.-T., Gu, B.-Y., & Ryu, G.-H. (2021). Influence of extrusion process parameters on specific mechanical energy and physical properties of high-moisture meat analog. *International Journal of Food Engineering*, *17*(2), 149–157. https://doi.org/10.1515/ijfe-2020-0042

Morales Alvarez, J. C. (2020). Engineering aspects of extrusion: Extrusion processing as a multiple-input and multiple-output system. *Extrusion Cooking*, 29–71. https://doi.org/10.1016/B978-0-12-815360-4.00002-X

Mościcki, L., & van Zuilichem, D. J. (2011). Extrusion-Cooking and Related Technique. In *Extrusion-Cooking Techniques* (pp. 1–24). Wiley. https://doi.org/10.1002/9783527634088.ch1

Osen, R., Toelstede, S., Eisner, P., & Schweiggert-Weisz, U. (2015). Effect of high moisture extrusion cooking on protein-protein interactions of pea (Pisum sativum L.) protein

isolates. *International Journal of Food Science and Technology*, *50*(6), 1390–1396. https://doi.org/10.1111/IJFS.12783

Osen, R., Toelstede, S., Wild, F., Eisner, P., & Schweiggert-Weisz, U. (2014). High moisture extrusion cooking of pea protein isolates: Raw material characteristics, extruder responses, and texture properties. *Journal of Food Engineering*, *127*, 67–74.

Palanisamy, M., Franke, K., Berger, R. G., Heinz, V., & Töpfl, S. (2019). High moisture extrusion of lupin protein: influence of extrusion parameters on extruder responses and product properties. *Journal of the Science of Food and Agriculture*, *99*(5), 2175–2185. https://doi.org/10.1002/JSFA.9410

Pietsch, V. L., Bühler, J. M., Karbstein, H. P., & Emin, M. A. (2019). High moisture extrusion of soy protein concentrate: Influence of thermomechanical treatment on protein-protein interactions and rheological properties. *Journal of Food Engineering*, *251*, 11–18. https://doi.org/10.1016/J.JFOODENG.2019.01.001

Pietsch, V. L., Emin, M. A., & Schuchmann, H. P. (2017). Process conditions influencing wheat gluten polymerization during high moisture extrusion of meat analog products. *Journal of Food Engineering*, *198*, 28–35. https://doi.org/10.1016/J.JFOODENG.2016.10.027

Prak, K. (2006). *Studies on structure-function relationships of soybean glycinin at subunit levels and improvement of its functions by protein engineering*. Kyoto University.

Rasheed, F., Markgren, J., Hedenqvist, M., & Johansson, E. (2020). Modeling to Understand Plant Protein Structure-Function Relationships—Implications for Seed Storage Proteins. *Molecules*, *25*(4), 873. https://doi.org/10.3390/molecules25040873

Rezaei, M., Shadizadeh, S. R., Vosoughi, M., & Kharrat, R. (2014). An experimental investigation of sequential CO2 and N2 Gas Injection as a new EOR method. *Energy Sources, Part A: Recovery, Utilization, and Environmental Effects*, *36*(17), 1938–1948. https://doi.org/10.1080/15567036.2011.557705

Riaz, M. N. (2000). *Introduction to Extruders and Their Principles*. 1–23. https://doi.org/10.1201/9781482278859-1

Rizvi, S. S. H., Mulvaney, S. J., & Sokhey, A. S. (1995). The combined application of supercritical fluid and extrusion technology. *Trends in Food Science & Technology*, *6*(7), 232–240. https://doi.org/10.1016/S0924-2244(00)89084-6

Rokkonen, T., Willberg-Keyriläinen, P., Ropponen, J., & Malm, T. (2021). Foamability of Cellulose Palmitate Using Various Physical Blowing Agents in the Extrusion Process. *Polymers*, *13*(15), 2416. https://doi.org/10.3390/polym13152416

Ryu, G.-H. (2020). Extrusion cooking of high-moisture meat analogues. In *Extrusion Cooking* (pp. 205–224). Elsevier. https://doi.org/10.1016/b978-0-12-815360-4.00007-9

Saldanha do Carmo, C., Knutsen, S. H., Malizia, G., Dessev, T., Geny, A., Zobel, H., Myhrer, K. S., Varela, P., & Sahlstrøm, S. (2021). Meat analogues from a faba bean concentrate can be generated by high moisture extrusion. *Future Foods*, *3*, 100014. https://doi.org/10.1016/J.FUFO.2021.100014

Samard, S., Gu, B. Y., & Ryu, G. H. (2019). Effects of extrusion types, screw speed and addition of wheat gluten on physicochemical characteristics and cooking stability of meat analogues. *Journal of the Science of Food and Agriculture*, *99*(11), 4922–4931. https://onlinelibrary.wiley.com/doi/abs/10.1002/jsfa.9722

Sandoval, M. J. L., Osen, R., Hiermaier, S., & Ganzenmüller, G. (2019). Towards understanding the mechanism of fibrous texture formation during high-moisture extrusion of meat substitutes. *Journal of Food Engineering*, *242*, 8–20. https://doi.org/10.1016/j.jfoodeng.2018.08.009

Schlangen, M., Ribberink, M. A., Taghian Dinani, S., Sagis, L. M. C., & van der Goot, A. J. (2023). Mechanical and rheological effects of transglutaminase treatment on dense plant protein blends. *Food Hydrocolloids*, *136*, 108261. https://doi.org/10.1016/j.foodhyd.2022.108261

Schmid, E., Farahnaky, A., Adhikari, B., & Torley, P. J. (2022). High moisture extrusion cooking of meat analogs: A review of mechanisms of protein texturization. *Comprehensive Reviews in Food Science and Food Safety*, *21*(6), 4573–4609. https://doi.org/10.1111/1541-4337.13030

Schreuders, F. K. G., Dekkers, B. L., Bodnár, I., Erni, P., Boom, R. M., & van der Goot, A. J. (2019). Comparing structuring potential of pea and soy protein with gluten for meat analogue preparation. *Journal of Food Engineering*, *261*, 32–39. https://doi.org/10.1016/j.jfoodeng.2019.04.022

Shand, P. J., Ya, H., Pietrasik, Z., & Wanasundara, P. K. J. P. D. (2007). Physicochemical and textural properties of heat-induced pea protein isolate gels. *Food Chemistry*, *102*(4), 1119–1130. https://doi.org/10.1016/j.foodchem.2006.06.060

Singh, R. (2021). *Effects of particle size distribution and extrusion processing parameters on the techno-functional properties of soybean meal* [University of Manitoba]. http://hdl.handle.net/1993/35749

Sun, C., Fu, J., Chang, Y., Li, S., & Fang, Y. (2022). Structure Design for Improving the Characteristic Attributes of Extruded Plant-Based Meat Analogues. *Food Biophysics*, *17*(2), 137–149. https://doi.org/10.1007/s11483-021-09692-w

Swain, S. N., Biswal, S. M., Nanda, P. K., & Nayak, P. L. (2004). Biodegradable Soy-Based Plastics: Opportunities and Challenges. *Journal of Polymers and the Environment*, *12*(1), 35–42. https://doi.org/10.1023/B:JOOE.0000003126.14448.04

Tay, S. L., Xu, G. Q., & Perera, C. O. (2005). Aggregation profile of 11S, 7S and 2S coagulated with GDL. *Food Chemistry*, *91*(3), 457–462. https://doi.org/10.1016/j.foodchem.2004.06.027

Thrane, M., Paulsen, P. V., Orcutt, M. W., & Krieger, T. M. (2017). Soy protein: Impacts, production and applications. In *Sustainable Protein Sources* (pp. 23–45). Elsevier. https://doi.org/10.1016/B978-0-12-802778-3.00002-0

Tolstoguzov, V. B. (1993). Thermoplastic extrusion-the mechanism of the formation of extrudate structure and properties. *Journal of the American Oil Chemists' Society*, *70*(4), 417–424. https://doi.org/10.1007/BF02552717

Vatansever, S., Tulbek, M. C., & Riaz, M. N. (2020a). Low- and High-Moisture Extrusion of Pulse Proteins as Plant-Based Meat Ingredients: A Review. *Cereal Foods World*, *65*(4). https://doi.org/10.1094/CFW-65-4-0038

Vatansever, S., Tulbek, M. C., & Riaz, M. N. (2020b). Low- and High-Moisture Extrusion of Pulse Proteins as Plant-Based Meat Ingredients: A Review. *Cereal Foods World*, *65*(4). https://doi.org/10.1094/CFW-65-4-0038

Webb, D., Li, Y., & Alavi, S. (2023). Chemical and physicochemical features of common plant proteins and their extrudates for use in plant-based meat. *Trends in Food Science & Technology, 131*, 129–138. https://doi.org/10.1016/j.tifs.2022.11.006

Wild, F. (2016). Manufacture of Meat Analogues Through High Moisture Extrusion. In *Reference Module in Food Science*. Elsevier. https://doi.org/10.1016/b978-0-08-100596-5.03281-9

Wittek, P., Ellwanger, F., Karbstein, H. P., & Emin, M. A. (2021). Morphology Development and Flow Characteristics during High Moisture Extrusion of a Plant-Based Meat Analogue. *Foods*, *10*(8), 1753. https://doi.org/10.3390/foods10081753

Wittek, P., & Emin, M. A. (2017). Three-Dimensional Modeling of Food Extrusion Processes. In *Reference Module in Food Science*. Elsevier. https://doi.org/10.1016/B978-0-08-100596-5.21211-0

Wittek, P., Karbstein, H. P., & Emin, M. A. (2021a). Blending Proteins in High Moisture Extrusion to Design Meat Analogues: Rheological Properties, Morphology Development and Product Properties. *Foods 2021, Vol. 10, Page 1509*, *10*(7), 1509. https://doi.org/10.3390/FOODS10071509

Wittek, P., Karbstein, H. P., & Emin, M. A. (2021b). Blending Proteins in High Moisture Extrusion to Design Meat Analogues: Rheological Properties, Morphology Development and Product Properties. *Foods*, *10*(7), 1509. https://doi.org/10.3390/foods10071509

Wittek, P., Zeiler, N., Karbstein, H. P., & Emin, M. A. (2021). High Moisture Extrusion of Soy Protein: Investigations on the Formation of Anisotropic Product Structure. *Foods*, *10*(1), 102. https://doi.org/10.3390/foods10010102

Wolf, W. J. (1970). Soybean proteins. Their functional, chemical, and physical properties. *Journal of Agricultural and Food Chemistry*, *18*(6), 969–976. https://doi.org/10.1021/jf60172a025

Yang, J., Zamani, S., Liang, L., & Chen, L. (2021). Extraction methods significantly impact pea protein composition, structure and gelling properties. *Food Hydrocolloids*, *117*, 106678. https://doi.org/10.1016/J.FOODHYD.2021.106678

Zahari, I., Ferawati, F., Helstad, A., Ahlström, C., Östbring, K., Rayner, M., & Purhagen, J. K. (2020). Development of High-Moisture Meat Analogues with Hemp and Soy Protein Using Extrusion Cooking. *Foods 2020, Vol. 9, Page 772*, *9*(6), 772. https://doi.org/10.3390/FOODS9060772

Zahari, I., Ferawati, F., Purhagen, J. K., Rayner, M., Ahlström, C., Helstad, A., & Östbring, K. (2021). Development and Characterization of Extrudates Based on Rapeseed and Pea Protein Blends Using High-Moisture Extrusion Cooking. *Foods 2021, Vol. 10, Page 2397*, *10*(10), 2397. https://doi.org/10.3390/FOODS10102397

Zahari, I., Östbring, K., Purhagen, J. K., & Rayner, M. (2022). Plant-Based Meat Analogues from Alternative Protein: A Systematic Literature Review. *Foods*, *11*(18), 2870. https://doi.org/10.3390/foods11182870

Zhang, B., Kang, X., Cheng, Y., Cui, B., & Abd El-Aty, A. M. (2022). Impact of high moisture contents on the structure and functional properties of pea protein isolate during extrusion. *Food Hydrocolloids*, *127*, 107508. https://doi.org/10.1016/J.FOODHYD.2022.107508

Zhang, J., Liu, L., Jiang, Y., Faisal, S., & Wang, Q. (2020). A new insight into the high-moisture extrusion process of peanut protein: From the aspect of the orders and amount of energy

input. *Journal of Food Engineering*, *264*, 109668. https://doi.org/10.1016/J.JFOODENG.2019.07.015

Zhang, J., Liu, L., Liu, H., Yoon, A., Rizvi, S. S. H., & Wang, Q. (2018). Changes in conformation and quality of vegetable protein during texturization process by extrusion. *Https://Doi-Org.Uml.Idm.Oclc.Org/10.1080/10408398.2018.1487383*, *59*(20), 3267–3280. https://doi.org/10.1080/10408398.2018.1487383

Zhong, C., Feng, Y., & Xu, Y. (2023). Production of Fish Analogues from Plant Proteins: Potential Strategies, Challenges, and Outlook. *Foods*, *12*(3), 614. https://doi.org/10.3390/foods12030614

Chapter III: Impact of cooling die temperature and nitrogen gas injection on the physical quality of soy protein meat analogues

Contributions of Authors: A version of this chapter has been submitted to the journal "Innovative Food Science and Emerging Technology" for publication with authorship by Neeraj Ghanghas, Mohammad Nadimi, Jitendra Paliwal, and Filiz Koksel. The manuscript was titled "Gas-assisted high-moisture extrusion of soy-based meat analogues: Impacts of nitrogen pressure and cooling die temperature on density, texture and microstructure." Neeraj Ghanghas was responsible for conceptualization, investigation, methodology, data curation, formal analysis, writing, reviewing, and editing the original draft, as well as writing review and editing. Mohammad Nadimi reviewed the manuscript and provided advice to improve the manuscript. Jitendra Paliwal provided resources for analysis, supervised the research, reviewed the manuscript, and provided critical advice. Filiz Koksel was involved in conceptualization, methodology, supervision, reviewing the manuscript, and providing critical advice. Additionally, Filiz Koksel provided resources and secured funding for the project.

3.1. Materials and methods

3.1.1. Materials

Soy protein isolate (SUPRO® EX 45) and soy protein concentrate (Solcon F) were procured from Azelis Canada Inc. (Brampton, ON, Canada) and St. Charles Trading Inc. (Elgin, IL, USA), respectively. The two constituents were blended using a mixer (Hobart Food Equipment Canada, Toronto, ON, Canada) to produce a soy protein blend (SP) with a protein content of 75% (dry basis).

3.1.2. Proximate analyses

Protein content (N × 6.25) and moisture content of the SP were analyzed using AACC International methods 46-13 and 44–19.01, respectively (AACC International, 1999). The blend's crude fat and ash content were determined using the methods described by Min & Ellefson (2010) and Marshall (2010), respectively. Total carbohydrate content was subtracting the measured protein, fat, ash, and water from the total weight. All proximate analyses were performed in triplicates. The proximate composition of the SP was 75.1% protein, 2.8% fat, 3.3% ash, and 18.8% carbohydrates on a dry basis.

The moisture content of the fresh meat analogues was determined following AACC International method 44–19.01 with a modification in drying time (16 h) to reach constant weight (AACC International, 1999). The moisture content of freeze-dried and ground meat analogues was determined following AACC International method 44–19.01 (AACC International, 1999). The moisture content values of the fresh and freeze-dried meat analogues were later used to calculate the gas-free meat analogue density.

3.1.3. High-moisture extrusion cooking

Meat analogues were prepared using a lab scale co-rotating twin-screw extruder (MPF 19, APV Baker Ltd., Peterborough, UK) with a barrel length to screw diameter ratio of 25:1, using the screw configuration reported by Koksel & Masatcioglu (2018). A constant screw speed of 200 rpm, barrel temperature profile from the feeder to the die end of 60-80-115-125 °C, dry feed rate of 0.5 kg/h and water feed rate to achieve a target moisture content of 70% (wet basis) were used during extrusion. The extruder was equipped with a long cooling die (MPF 19 T.V.P. DIE, Baker Perkins, Peterborough, UK) having a length of 300 mm, a width of 50 mm and a spacer of 5 mm.

Extrusion was performed as a function of the long cooling die temperature (DT). Three DTs of 35 °C, 50 °C and 65 °C were selected to cover a wide range of temperatures typically used in the industry.

A gas injection assembly, equipped with a pressure gauge and a pressure regulator, connected to a nitrogen gas tank was installed onto the extruder barrel for gas-assisted extrusion. At each DT, three nitrogen gas injection pressures (GP) of 0 bar (i.e., conventional extrusion), 1 bar and 2.5 bar were studied. Extrusion runs were performed in triplicates for each extrusion DT-GP combination treatment. The torque values were noted upon achieving steady state extrusion conditions, and the specific mechanical energy (SME) input was calculated following the method of Singh & Koksel (2021) using equation 1:

$$SME\ \left({}^{Wh}/_{kg}\right) = \frac{\frac{actual\ screw\ speed}{\max screw\ speed} \times \frac{torque}{100} \times motor\ power}{mass\ flow\ rate} \qquad \text{(equation 1)}$$

For each DT-GP combination treatment (Table 3.1), meat analogues were collected in the form of ~20 cm long ribbons. A portion of the meat analogues was refrigerated to be tested for density, textural quality and microstructural attributes on the next day. The rest of the meat analogues were frozen, freeze-dried and then ground to be tested for gas-free meat analogue density.

3.1.4. Physical quality of meat analogues

3.1.4.1. Density of meat analogues

The density of meat analogues was determined using a 25 mL specific gravimetric bottle (LG-3542, SP Wilmad-LabGlass, Vineland, NJ, USA). Approximately 1 g of meat analogue sub-sample was cut using a pathology blade and precisely weighed using an analytical balance

(±0.0001 g). The density of the sub-sample was determined using the Koksel & Scanlon (2012) method in triplicates for each extrusion treatment replicate.

3.1.4.2. Texture

Textural properties of meat analogues were assessed using a texture analyzer (TA.XT plus, Stable Micro Systems, Godalming, UK). Texture profile analysis (TPA) was performed following the method of Diaz et al. (2022) with some modifications. Briefly, meat analogues were cut into square-shaped sub-samples of 20 mm × 20 mm (thickness: 5 mm). TPA was performed (n=5) using a cylindrical probe with a diameter of 38 mm. The hardness, gumminess, springiness, and chewiness values were recorded from each measurement.

The cutting strength of meat analogues in the longitudinal and transversal directions of meat analogue flow from the long cooling die was determined using the method of Guillermic et al. (2023). Square-shaped meat analogue sub-samples of 20 mm × 20 mm (thickness: 5 mm) were cut using a craft knife accessory (A/ECB probe, Stable Micro Systems, Godalming, UK). The peak cutting force in transversal (F_T) and longitudinal (F_L) directions (n=6) was recorded (Caporgno et al., 2020; Guillermic et al., 2023). The degree of texturization was determined by taking the ratio of F_T to F_L.

3.1.4.3. Microstructure

A bench-top X-ray micro-computed tomograph (Skyscan 1275, Bruker, Zaventem, Belgium) was used to characterize the microstructure of the meat analogues. Meat analogues were cut into rectangular sub-samples of 1 cm × 3 cm (thickness: 5 mm) and wrapped using saran wrap to prevent moisture loss during image acquisition. X-ray projection images were acquired at a rotation angle of 0.2° over 180° with an exposure time of 48 ms at each rotation angle. For image

acquisitions, the values of pixel size, source current, source voltage and frame averaging were set at 9 µm, 250 µA, 40 kV and 9, respectively, based on preliminary trials that optimized noise level and pixel size.

NRecon software (Bruker, Zaventem, Belgium) was used to reconstruct 700 2D cross-sectional images from the X-ray tomography projections. CTAn software package (Bruker, Zaventem, Belgium) was used to crop the 2D images to the size 780 × 450 pixels and binarize cropped images by selecting a grey level value (threshold value). This threshold value defined the boundaries between the bubbles (i.e., gas cells) and the solid protein-rich matrix. The threshold values during the binarization process were objectively determined in a way that allowed the matching of the gas volume fraction obtained from density measurements ($\emptyset_{density}$, equation 2) with the gas volume fraction obtained from X-ray microtomography ($\emptyset_{X-ray}$, equation 3).

$$\emptyset_{density}\ (\%) = \left[1 - \frac{\rho_{Meat\ analogue}}{\rho_{Gas-free\ meat\ analogue}}\right] \times 100 \qquad \text{(equation 2)}$$

Where $\emptyset$ and ρ stands for gas volume fraction and density, respectively.

$$\emptyset_{X-ray} = \left[\frac{number\ of\ pixels\ in\ bubble\ cross\ sections}{total\ number\ of\ pixels\ in\ the\ analyzed\ 2D\ image}\right] \times 100 \qquad \text{(equation 3)}$$

For determining gas-free meat analogue density, meat analogues were freeze-dried, followed by grinding using a centrifugal mill (ZM 200, Retsch, Haan, Germany) with a sieve size of 250 microns. The density of the ground gas-free meat analogues was measured using a pycnometer following the method of Luo et al. (2020) using equation 4.

$$\rho_{Gas-free\ meat\ analogue} = (\rho_{water} \times X_{water}) + (\rho_{protein} \times X_{protein}) \qquad \text{(equation 4)}$$

Where X stands for the mass fractions of water or protein in the meat analogues.

The binarized 2D images were then stacked together to create 3D voxels (780 × 450 × 700 pixels^3) using the CTvox software package (Bruker, Zaventem, Belgium). These voxels were analyzed using CTAn software package (Bruker, Zaventem, Belgium) to obtain (1) major diameter (in µm) of the bubbles, (2) sphericity of the bubbles, and (3) maximum structure thickness (in µm) of the bubbles, where the latter is defined as the diameter of the largest sphere that fits inside that bubble (Germishuys & Manley, 2021). These analyses were only performed for the meat analogues produced at 2.5 bar nitrogen gas injection pressure because no bubbles were observed at 0 and 1 bar nitrogen gas injection pressures (Appendix 1), possibly due to the image resolution limitations of the X-ray micro-computed tomograph.

3.1.5. Statistical analysis

The data were analyzed using one-way ANOVA and the Tukey test ($p<0.05$) using the OriginPro software package (Version 2023).

3.2. Results and Discussion

3.2.1. Effects of cooling die temperature (DT) and nitrogen gas injection pressure (GP) on torque and specific mechanical energy (SME) input

The effects of DT and GP on torque and SME input during extrusion are presented in Table 3.1. The SME input values required to texturize soy proteins averaged 55.9 Wh/kg and concurred with previously published literature (Mateen et al., 2023; Pietsch et al., 2019).

An increase in GP from 0 to 1 bar at a given DT resulted in a decrease or no significant change in the torque and SME input values. However, when the gas injection pressure was further increased to 2.5 bar, the torque and SME input values increased significantly ($p < 0.05$). This significant ($p < 0.05$) rise in torque and SME values could be due to an increase in the fill of the extruder barrel (Akdogan, 1996; Sato et al., 1999) caused by the higher level of nitrogen gas injection pressure, as the GP is positively related to the gas flow rate. At a given GP, a decrease in the DT from 65 °C to 35 °C led a significant increase ($p < 0.05$) in the torque and SME input values. This increase, as DT decreases, could be due to the augmented hindrance to the melt flow from the extruder barrel to the die brought about by the increased melt viscosity at lower temperatures (Akdogan, 1996; Diaz et al., 2022) inside the long cooling die.

Table 3.1: Effects of long cooling die temperature (DT) and nitrogen gas injection pressure (GP) on the torque and specific mechanical energy (SME) input during high-moisture extrusion cooking.

Meat analogue extrusion conditions			
DT (°C)	Pressure (Bar)	Torque (%)	SME (Wh/kg)
35	0	11.3 ± 0.3^{b}	59.7 ± 1.5^{b}
50	0	10.3 ± 0.1^{c}	54.5 ± 0.8^{c}
65	0	9.9 ± 0.1^{cd}	52.3 ± 0.8^{cd}
35	1	9.7 ± 0.4^{d}	50.9 ± 2.0^{d}
50	1	10.0 ± 0.0^{cd}	52.7 ± 0.0^{cd}
65	1	9.0 ± 0.0^{e}	47.4 ± 0.0^{e}
35	2.5	12.3 ± 0.3^{a}	64.6 ± 1.3^{a}
50	2.5	12.0 ± 0.0^{a}	63.2 ± 0.0^{a}
65	2.5	11.0 ± 0.0^{b}	58.0 ± 0.0^{b}

Torque and SME input values are reported as the mean ± standard deviation, n = 3. For each column, values that do not share a letter are significantly different ($p < 0.05$).

3.2.2. Effects of DT and GP on meat analogue density

The density is a primary indicator of air content in aerated food products (Campbell, 1999). The effects of DT and GP on the density of meat analogues are presented in Figure 3.1. The density of meat analogues varied between 1070 and 1111 kg/m^3, in agreement with those reported by Högg & Rauh (2023) for meat analogues made from soy protein at 70% moisture content. A significant variation in density was observed between the meat analogues produced at different combinations of DT and GP. The introduction of air or gas during food processing (e.g., dough mixing) causes the entrapment of bubbles in the food matrix, creating an aerated food structure, which directly influences food's density (Awuchi et al., 2019; Campbell, 1999). Accordingly, the variation in density of the meat analogues was likely due to the variation in the amount of nitrogen gas entrapped and held in their matrix. For all three cooling DTs studied, as the GP increased, meat analogue density decreased. This decrease was highest for the lowest cooling die temperature (i.e., 35 °C).

Under the extrusion conditions studied, the lowest density was found for the meat analogues produced at the treatment combination of the lowest DT (i.e., 35 °C) and the highest GP (i.e., 2.5 bar), indicating the highest gas volume fraction in these meat analogues. Overall, as the DT increased at a given GP, meat analogue density increased, indicating a lesser volume of gas being held in the meat analogues. This trend was the most evident and statistically significant ($p < 0.05$) for the highest GP, i.e., 2.5 bar. Higher processing temperatures can cause gas to escape from the protein matrix (Schreuders et al., 2019) increasing in the density of meat analogues.

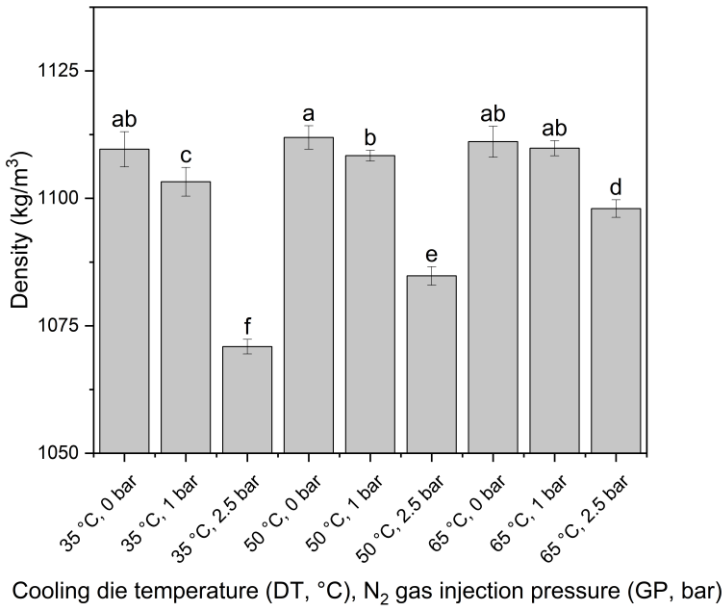

Figure 3.1: Density of the meat analogues produced at different long cooling die temperature (DT) and nitrogen gas injection pressure (GP) combinations. Error bars represent ± standard deviation, n = 9. Bars that do not share a letter differ significantly ($p < 0.05$).

3.2.3. Effects of DT and GP on microstructure

The gas volume fraction obtained from density measurements and X-ray microtomography ($\emptyset_{X-ray}$) as a function of DT is reported in Table 3.2 for the meat analogues produced at 2.5 bar GP. Overall, the gas volume fraction of the meat analogues ranged from approximately 2.8 to 5.5%. To our knowledge, this is the first report of the gas volume fraction in plant-based meat analogues produced using high-moisture extrusion. For shear-cell-produced plant-based meat analogues at similar moisture content levels and processing temperatures, a roughly close gas volume fraction (0.1-7%) was reported (Schreuders et al., 2019). The meat analogues produced at 65 °C DT had

the lowest gas volume entrapped in their matrix. These findings agree with Schreuders et al. (2019) who reported that higher processing temperatures can cause gas to escape from protein matrices.

Table 3.2: Gas volume fraction in meat analogues determined by density ($Ø_{density}$) and by X-ray microtomography ($Ø_{X-ray}$) analyses.

Meat analogue extrusion conditions			
DT (°C)	GP (Bar)	$Ø_{density}$±SE[a] (%)	$Ø_{X-ray}$±SE[b] (%)
35	2.5	4.4 ± 2.4[a]	4.4 ± 0.0[b]
50	2.5	5.4 ± 1.0[a]	5.5 ± 0.1[a]
65	2.5	2.9 ± 0.5[a]	2.8 ± 0.0[c]

SE[a] = Standard error (calculated by the propagation of errors), n = 3; SE[b] = Standard error, n = 3. For each column, values that do not share a letter are significantly different ($p < 0.05$).

The 3D individual bubble analyses provided important characteristics of the bubbles, i.e., maximum structure thickness, major diameter and sphericity. The histogram distribution of the maximum structure thickness of the meat analogues is presented in Figure 3.2. On average, the maximum structure thickness increased with an increase in DT, as the meat analogues produced at 65 °C had a relatively higher frequency of bubbles with maximum structure thickness ≥ 30 µm than those at lower DT conditions. The average maximum structure thickness is often related to the mechanical properties of foods (Trater et al., 2005) like bread (Germishuys & Manley, 2021;

Scanlon & Zghal, 2001) and extruded puffed snacks (Altan & Yağci, 2023; Trater et al., 2005). Increasing maximum structure thickness increases the hardness and toughness of aerated foods such as cake (Sozer et al., 2011). In line with these, our texture measurements revealed that the longitudinal and transverse cutting forces and hardness were the most for the highest DT meat analogues when averaged over all the GP conditions studied (see section 3.4).

The major diameter distribution of the bubbles in the meat analogues produced at DT conditions was lognormal (Figure 3.3). The lognormal distribution of meat analogues produced at 35 °C, 50 °C, and 65 °C DT had median diameters of 55.6±0.7, 54.2±0.5 and 49.6±1.7 µm, respectively, and widths of 890.6±12.2, 835.2±7.4 and 661.2±17.2 µm, respectively. The median and the width of the lognormally distributed meat analogue major bubble diameter decreased with an increase in the DT. The 2D visualization presented in Figure 3.4 also shows that compared to higher DT meat analogues (i.e., 65 °C), larger bubbles were present in the meat analogues produced at lowest DT (i.e., 35 °C). These results suggest that the variation of bubble sizes in a meat analogue depends on the choice of DT and the lower the DT, the larger and more diverse the bubbles.

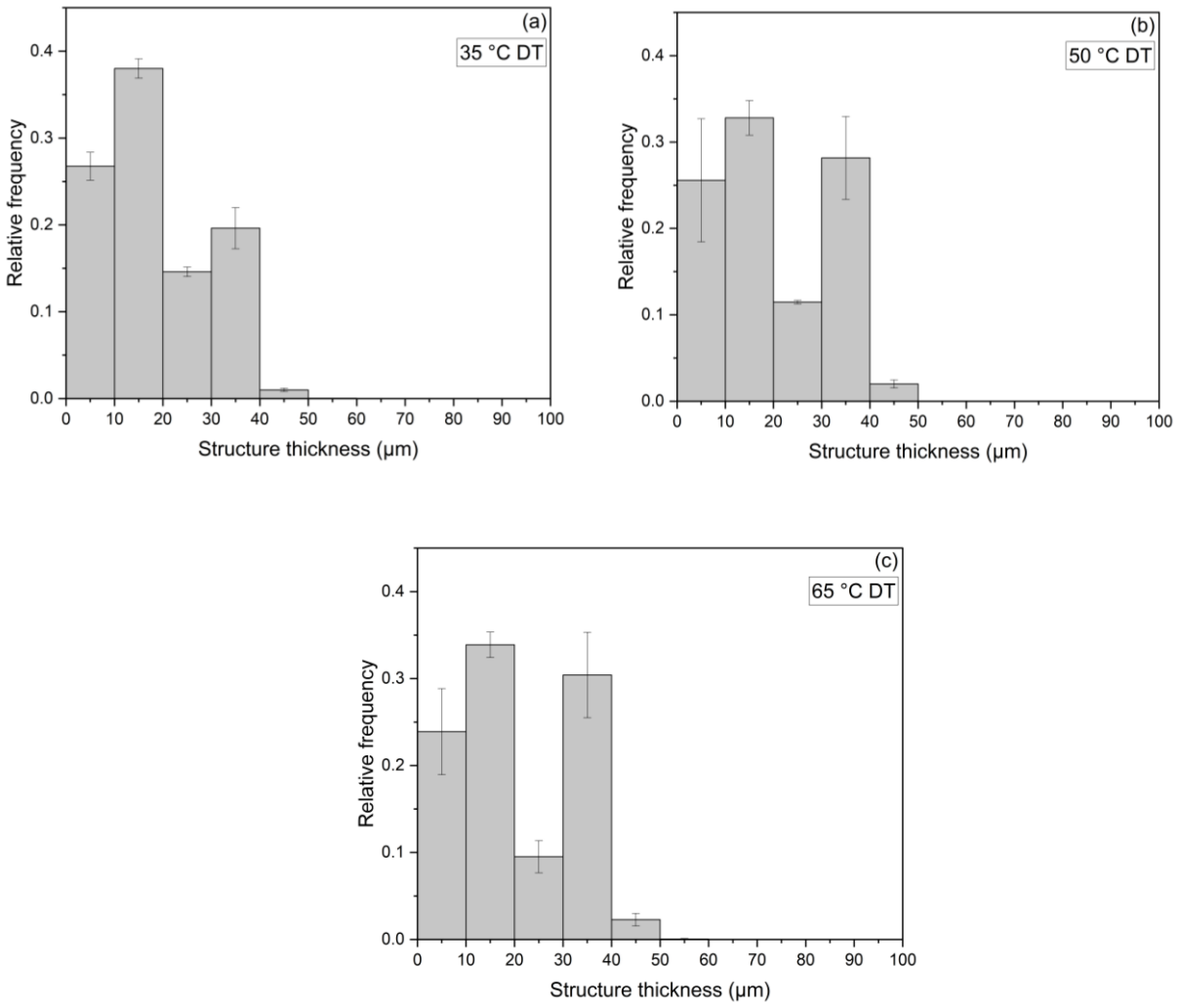

Figure 3.2: The histogram distribution of maximum structure thickness of bubbles in meat analogues produced at nitrogen gas injection pressure (GP) of 2.5 bar and cooling die temperatures (DT) of (a) 35 °C, (b) 50 °C, and (c) 65 °C. Error bars represent ± standard deviation, n = 3.

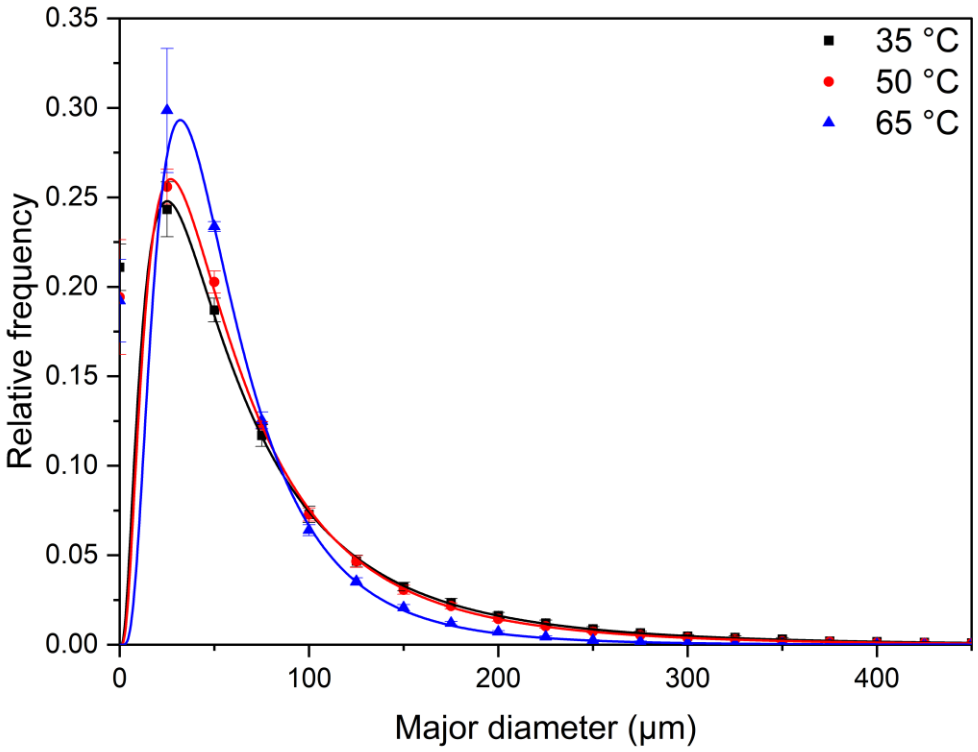

Figure 3.3: Lognormal distribution function fit for the major diameter of bubbles in meat analogues produced at 2.5 bar nitrogen gas injection pressure (GP), n = 3. The fit equations for the 35 °C, 50 °C, and 65 °C long cooling die temperatures (DT) are $y = \frac{20.7}{\sqrt{2\pi}\times 0.9\times x} exp\left[\frac{\left[ln\frac{x}{55.6}\right]^2}{2\times 0.9^2}\right]$, $y = \frac{20.8}{\sqrt{2\pi}\times 0.8\times x} exp\left[\frac{\left[ln\frac{x}{54.2}\right]^2}{2\times 0.8^2}\right]$, and $y = \frac{19.4}{\sqrt{2\pi}\times 0.7\times x} exp\left[\frac{\left[ln\frac{x}{49.6}\right]^2}{2\times 0.7^2}\right]$, respectively.

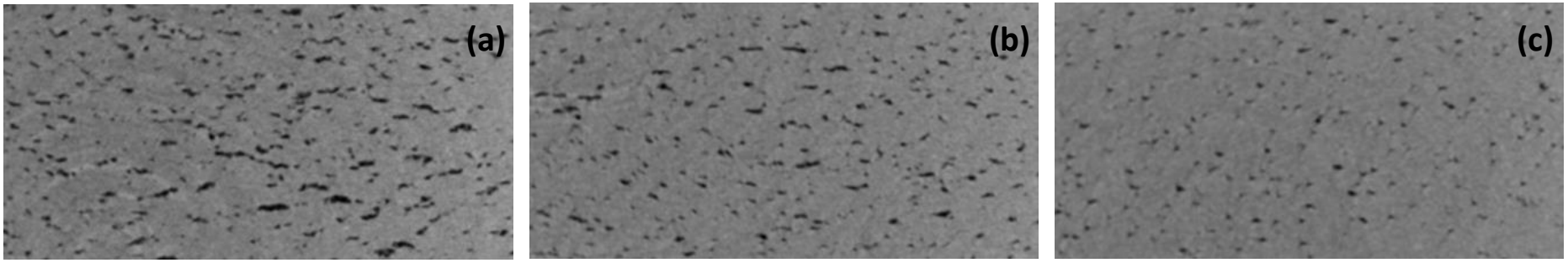

Figure 3.4: 2D reconstructed cross sectional slices of meat analogues produced at nitrogen gas injection pressure (GP) of 2.5 bar and long cooling die temperature (DT) of (a) 35 °C, (b) 50 °C and (c) 65 °C. The black color represents the bubbles, and the grey color represents the meat analogue matrix surrounding the bubbles. The size of each slice is approximately 4 mm × 2 mm.

The histogram distribution of the bubble sphericity is presented in Figure 3.5. The mean sphericity of bubbles in meat analogues produced at 35 °C, 50 °C, and 65 °C DT were 0.76±01, 0.78±0.01, and 0.81±0.02, respectively. The sphericity of bubbles at all three DT conditions showed a skewed distribution to the left. Since sphericity can have a maximum value of one, representing a perfectly spherical shape (Wadell, 1935), these <1 mean sphericity values indicated that the bubble shapes deviated from the shape of a perfect sphere.

The mean sphericity values increased with an increase in DT, and the mean sphericity of 35 °C DT was significantly ($p < 0.05$) lower than those of 50 °C and 65 °C. Overall, the meat analogues produced at 65 °C DT resulted in a relatively higher frequency of bubbles with sphericity values ≥ 0.8 than those produced at lower DT. The change in bubble sphericity with variation in DT could be due to the change in the parabolic flow profile of the melt in the long cooling die, which primarily depends on melt viscosity (Wittek, Karbstein, et al., 2021; Wittek, Zeiler, et al., 2021). It is well known that temperature can significantly influence the viscosity of a liquid; the viscosity of the melt during extrusion increases with a decrease in temperature (De Angelis et al., 2023). The increase in the torque and SME input values with the decrease in DT (Table 3.1) also supports this finding. In the long cooling die, the viscosity of the melt is highest at the wall of the die (where the temperature is the lowest) and lowest at the hot core of the melt (where the temperature is the highest). This viscosity gradient across the cross-section of the cooling die depends on the temperature difference between the melt and the die wall (Wittek, Karbstein, et al., 2021; Wittek, Zeiler, et al., 2021). The melt flow profile elongates as the melt flows along the long cooling die (De Angelis et al., 2023; Wittek, Karbstein, et al., 2021; Wittek, Zeiler, et al., 2021), and therefore it is expected that bubbles also elongate with the flow and lose their sphericity during melt solidification.

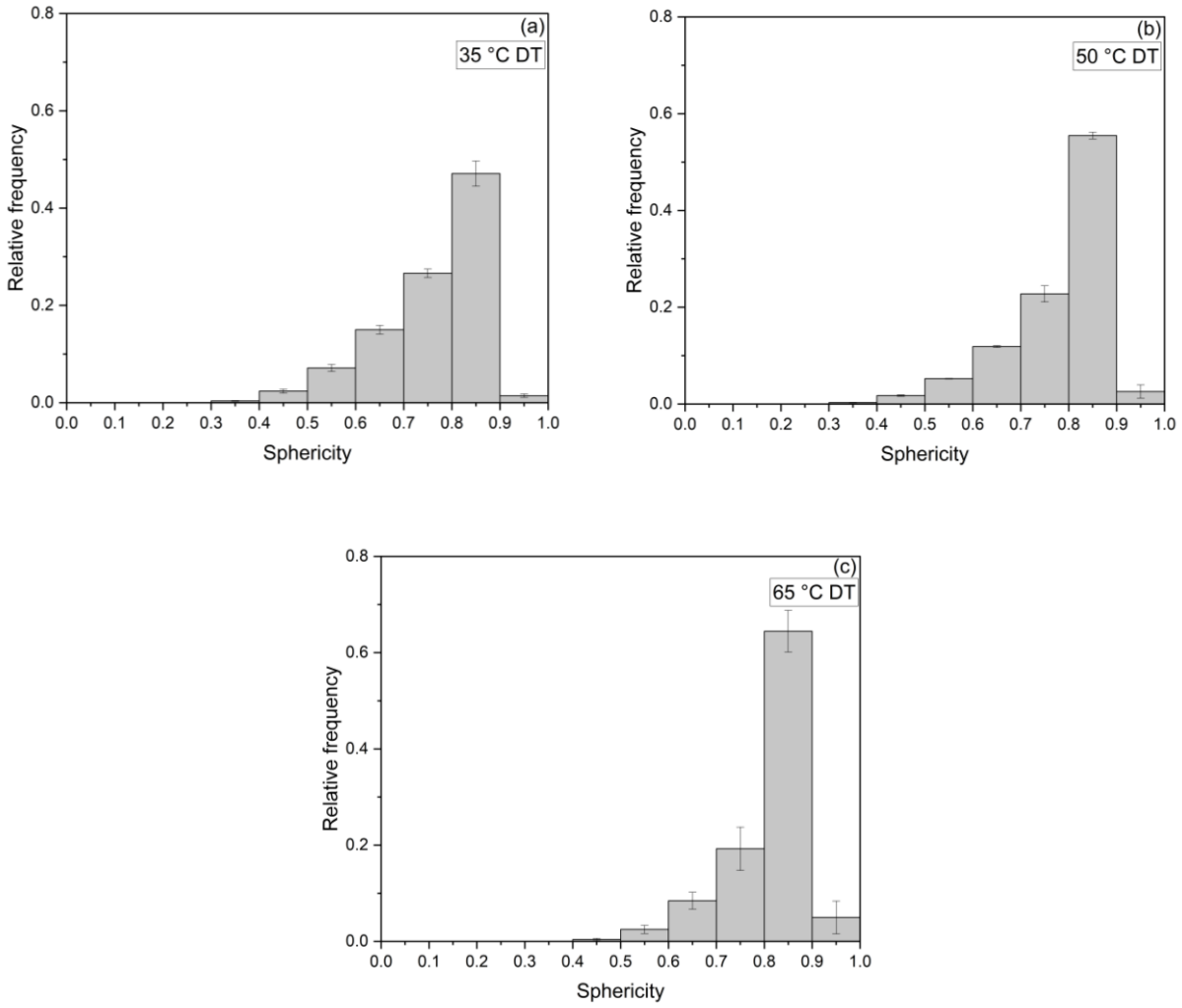

Figure 3.5: The histogram distribution of the sphericity of bubbles in the meat analogues produced at nitrogen gas injection pressure (GP) of 2.5 bar and cooling die temperatures (DT) of (a) 35 °C, (b) 50 °C, and (c) 65 °C. Error bars show ± standard deviation, n = 3.

3.2.4. Effects of DT and GP on meat analogue texture

The transversal (F_T) and longitudinal (F_L) peak cutting forces were in the range of 3.97-5.79 N and 3.73-6.00 N, respectively (Figure 3.6a and b). Overall, at a given constant GP, an increase in DT led to an increase in both F_T and F_L values. Diaz et al. (2022), who studied texturization of oat fiber-pea protein blends, also reported an increase in F_T and F_L values with an increase in long cooling die temperature in a similar range (40 °C-80 °C) and explained the high F_T and F_L values with changes in protein texturization and orientation of the fibrous structures in meat analogues. In addition to the possible changes in the fibre orientation with cooling die temperature, our microstructure analysis revealed that as DT increased, meat analogue density increased. Thus, the gas volume fraction in these meat analogues decreased (i.e., denser meat analogue), which may also be responsible for the observed increase in F_T and F_L values.

At a constant DT, no clear trend was observed for F_T and F_L values with a change in GP. When different combinations of DT and GP were compared, the lowest F_L was observed for the meat analogues produced at 35 °C DT and 1 bar GP and the highest F_L for 65 °C DT and 2.5 bar GP. These results suggest that different combinations of DT and GP can provide more flexibility to manipulate the textural quality attributes of meat analogues.

The degree of texturization (the ratio of F_T to F_L) for all meat analogues except for those produced using 65 °C DT and 2.5 bar GP had a value > 1 (Figure 3.6c), suggesting that the alignment of fibres is more in the longitudinal direction than in the transverse direction (Ferawati et al., 2021). Overall, the degree of texturization results agree with those reported by Lee et al. (2023) for meat analogues made from soy proteins. The difference between F_T and F_L implies texturization of soy protein; a greater difference between these forces means higher protein texturization (Osen et al., 2014). Based on Figure 3.6c, the highest texturization level, albeit

statistically insignificant ($p > 0.05$), was observed for the meat analogues produced at 35 °C DT and 2.5 bar GP. In addition, the degree of texturization values of meat analogues produced under most extrusion conditions in this study was close to those values reported for chicken breast and chicken drumstick by Mazlan et al. (2020).

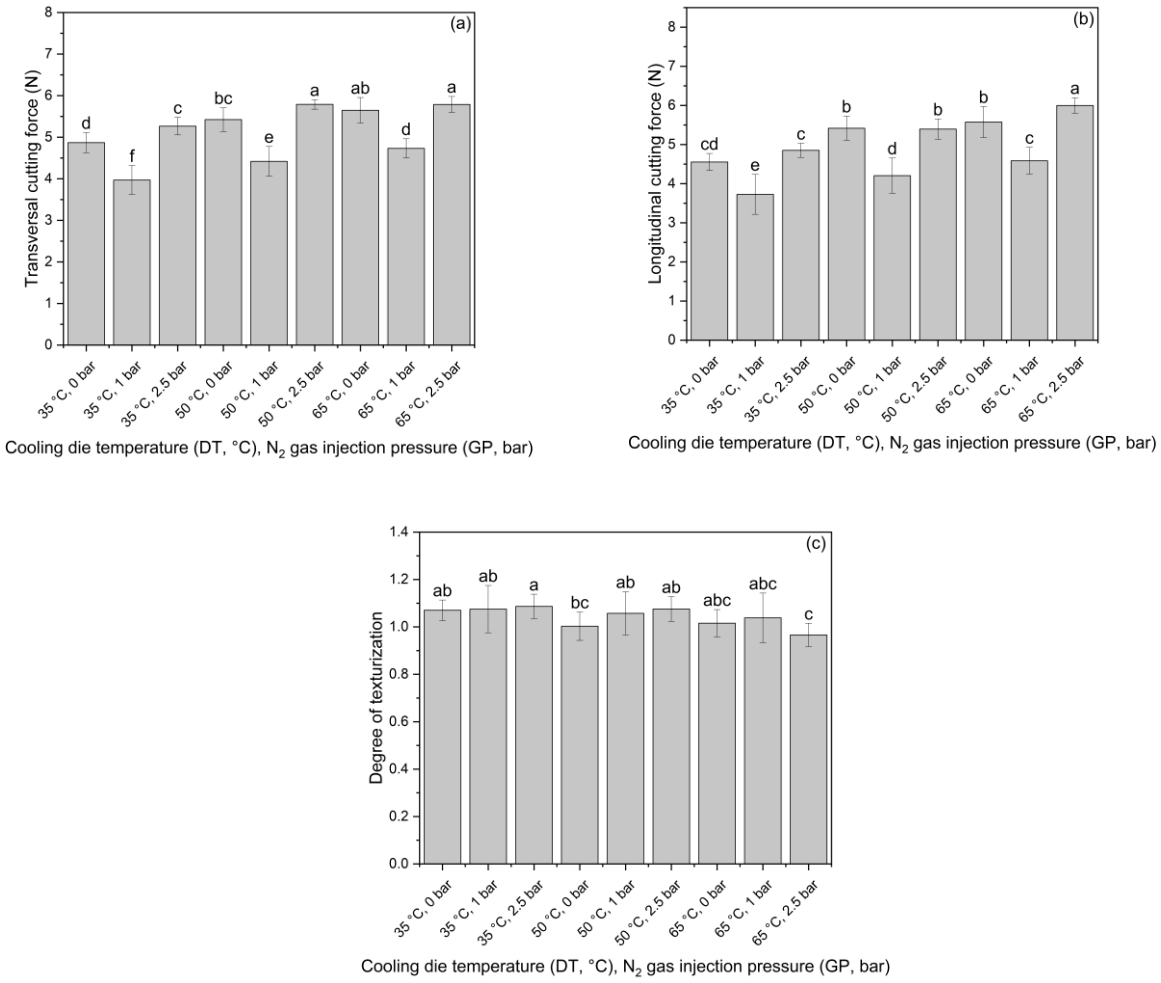

Figure 3.6: The transversal cutting force (a), longitudinal cutting force (b), and degree of texturization (c) of the meat analogues as a function of long cooling die temperature (DT) and nitrogen gas injection pressure (GP). Error bars show ± standard deviation, n = 18. The bars that do not share a letter differ significantly ($p < 0.05$).

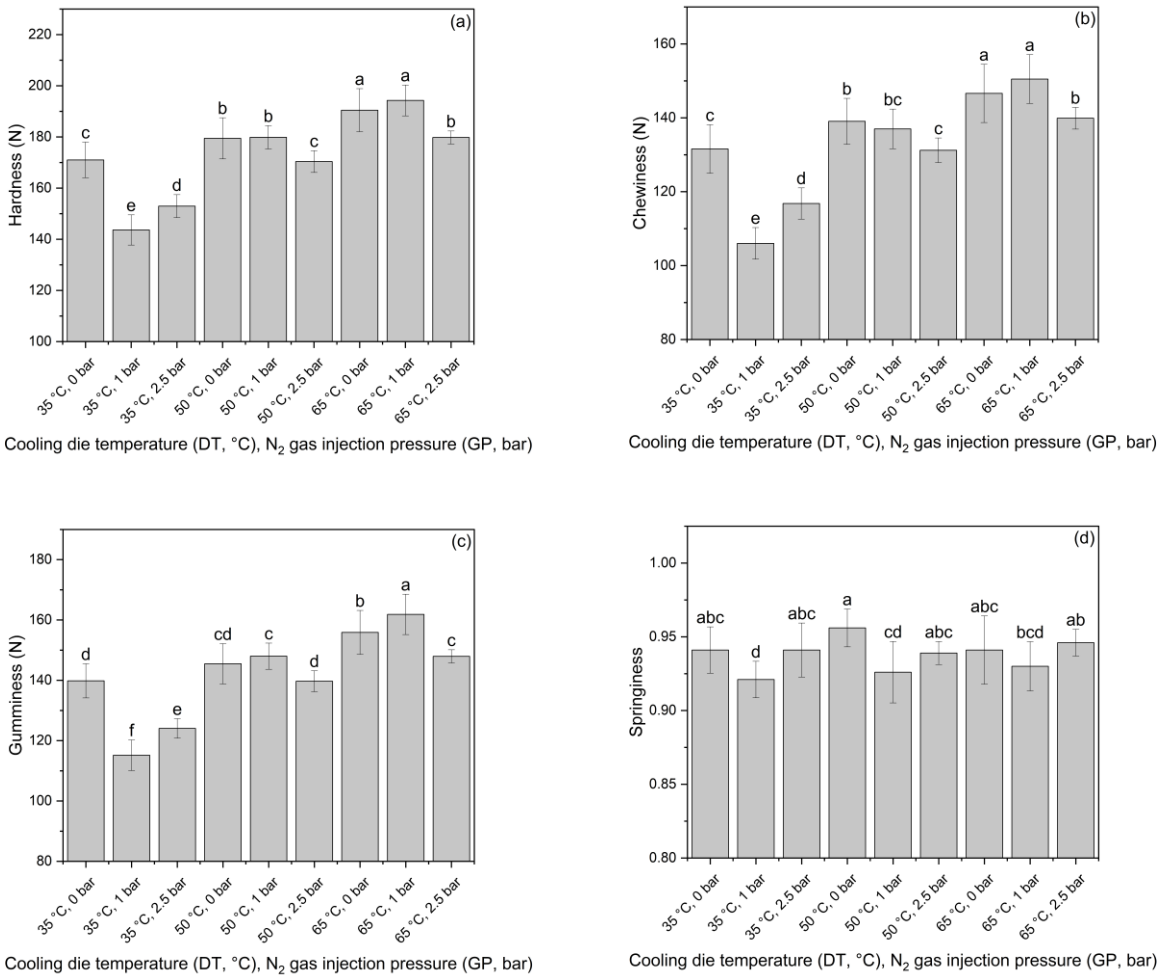

Figure 3.7: The texture profile analysis results (a) hardness, (b) chewiness, (c) gumminess, and (d) springiness of meat analogues as a function of long cooling die temperature (DT) and nitrogen gas injection pressure (GP). The error bars denote ± standard deviation, n = 15. The bars that do not share a letter differ significantly ($p < 0.05$).

The texture profile analysis results are presented in Figure 3.7. The combination of the lowest DT and the medium (i.e., 1 bar) GP resulted in meat analogues with the lowest hardness, chewiness, and gumminess values. The effect of nitrogen gas injection on the hardness, chewiness and gumminess of meat analogues was more prominent at the lowest DT i.e., 35 °C; the hardness, chewiness and gumminess values of meat analogues produced with nitrogen gas injection (GP of 1 and 2.5 bar) were significantly lower than that produced without nitrogen gas injection (0 bar). The presence of nitrogen gas in the meat analogue matrix due to nitrogen gas injection might have caused the decrease in the hardness, chewiness and gumminess values. The meat analogues produced at 35 °C DT and 1 and 2.5 bar GP had chewiness, gumminess and springiness values close to those of ham (Andronikov et al., 2013). In addition, the hardness values of meat analogues produced at 35 °C DT and 1 bar GP as well as 35°C DT and 2.5 bar GP were roughly close to those reported for beef by Conroy et al. (2017) and Dang et al. (2020). However, the values of other textural properties for these meat analogues were much higher than those of beef.

A closer look at the hardness, chewiness, and gumminess results revealed that irrespective of GP, an increase in DT resulted in a significant increase ($p < 0.05$) in the hardness, chewiness, and gumminess values of meat analogues, corroborating the results of Diaz et al. (2022). The hardness, chewiness, and gumminess values were highest for meat analogues produced at the highest DT when averaged over all GP conditions studied, but the torque and SME input values were the lowest. This observation could be explained by the lower viscosity of the melt at higher DTs; the lower melt viscosity not only minimizes torque and SME input values by facilitating a smoother flow of the melt from the barrel (Diaz et al., 2022) but also results in more elongated flow profile of the melt in the long cooling die, causing the fibres to orient longitudinally (Diaz et al., 2022; Osen et al., 2014; Wittek, Karbstein, et al., 2021; Wittek, Zeiler, et al., 2021). The

increase of fibre orientation in the longitudinal direction can cause an increase in the hardness of meat analogues. Since chewiness and gumminess values are directly proportional to hardness, an increase in chewiness and gumminess values can also be expected.

The results of the meat analogue microstructure and density (for those produced at 2.5 bar GP) were in line with the results of the texture profile analysis. For example, as the DT increased, meat analogue density significantly increased ($p < 0.05$), and so did the mean hardness, chewiness and gumminess. This increase was accompanied by an increase in the mean maximum structure thickness and the mean bubble sphericity, and a decrease in the mean major bubble diameter. The mechanical behaviour of cellular foods during compression depends on their cellular structure; during compression, bubbles (or cells) in an aerated food can deform, buckle or collapse depending on its cellular structure (Gibson & Ashby, 1988). Therefore, the observed variation in the texture profile of meat analogues produced with gas injection could be attributed to the change in their density and the characteristics of the bubbles in their matrix. Furthermore, given that the meat analogues produced at 65 °C DT and 2.5 bar GP had lower gas volume fraction and higher hardness, chewiness, and gumminess values than those produced at 35 °C DT and the same GP, it is not farfetched to conclude that the behaviour of meat analogues under compression (like during texture profile analysis) depends on their gas volume fraction. Overall, the microstructure and density results suggest that gas-assisted high-moisture extrusion can be used to manipulate the microstructure of plant-based meat analogues, providing a novel means to improve their textural characteristics.

References

AACC. (1999). *Approved methods of the American association of cereal chemists international* (11th ed.). AACC International.

Akdogan, H. (1996). Pressure, torque, and energy responses of a twin screw extruder at high moisture contents. In *Food Research International* (Vol. 29).

Altan, A., & Yağci, S. (2023). Physicochemical characteristics and structural changes of fermented faba bean extrudates prepared by twin-screw extrusion. *Food Chemistry*, *411*, 135502. https://doi.org/10.1016/j.foodchem.2023.135502

Andronikov, D., Gašperlin, L., Polak, T., & Žlender, B. (2013). Texture and Quality Parameters of Slovenian Dry-Cured Ham Kraški pršut According to Mass and Salt Levels. *Food Technology and Biotechnology*, *51*(1), 112–122.

Awuchi, C. G., Igwe, V. S., & Echeta, C. K. (2019). The functional properties of foods and flours. *International Journal of Advanced Academic Research*, *5*(11). http://www.ijaar.org/articles/Volume5-Number11/Sciences-Technology-Engineering/ijaar-ste-v5n11-nov19-p16.pdf

Campbell, G. (1999). Creation and characterisation of aerated food products. *Trends in Food Science & Technology*, *10*(9), 283–296. https://doi.org/10.1016/S0924-2244(00)00008-X

Caporgno, M. P., Böcker, L., Müssner, C., Stirnemann, E., Haberkorn, I., Adelmann, H., Handschin, S., Windhab, E. J., & Mathys, A. (2020). Extruded meat analogues based on yellow, heterotrophically cultivated Auxenochlorella protothecoides microalgae. *Innovative Food Science & Emerging Technologies*, *59*, 102275. https://doi.org/10.1016/j.ifset.2019.102275

Conroy, P. M., O' Sullivan, M. G., Hamill, R. M., & Kerry, J. P. (2017). Sensory capability of young, middle-aged and elderly Irish assessors to identify beef steaks of varying texture. *Meat Science*, *132*, 125–130. https://doi.org/10.1016/j.meatsci.2017.05.020

Dang, D. S., Buhler, J. F., Davis, H. T., Thornton, K. J., Scheffler, T. L., & Matarneh, S. K. (2020). Inhibition of mitochondrial calcium uniporter enhances postmortem proteolysis and tenderness in beef cattle. *Meat Science*, *162*, 108039. https://doi.org/10.1016/j.meatsci.2019.108039

De Angelis, D., Opaluwa, C., Pasqualone, A., Karbstein, H. P., & Summo, C. (2023). Rheological properties of dry-fractionated mung bean protein and structural, textural, and rheological evaluation of meat analogues produced by high-moisture extrusion cooking. *Current Research in Food Science*, *7*, 100552. https://doi.org/10.1016/j.crfs.2023.100552

Diaz, J. M. R., Kantanen, K., Edelmann, J. M., Suhonen, H., Sontag-Strohm, T., Jouppila, K., & Piironen, V. (2022). Fibrous meat analogues containing oat fiber concentrate and pea protein isolate: Mechanical and physicochemical characterization. *Innovative Food Science & Emerging Technologies*, *77*, 102954. https://doi.org/10.1016/J.IFSET.2022.102954

Ferawati, F., Zahari, I., Barman, M., Hefni, M., Ahlström, C., Witthöft, C., & Östbring, K. (2021). High-Moisture Meat Analogues Produced from Yellow Pea and Faba Bean Protein Isolates/Concentrate: Effect of Raw Material Composition and Extrusion Parameters on Texture Properties. *Foods 2021, Vol. 10, Page 843*, *10*(4), 843. https://doi.org/10.3390/FOODS10040843

Germishuys, Z., & Manley, M. (2021). X-ray micro-computed tomography evaluation of bubble structure of freeze-dried dough and foam properties of bread produced from roasted wheat

flour. *Innovative Food Science & Emerging Technologies*, *73*, 102766. https://doi.org/10.1016/j.ifset.2021.102766

Gibson, L. J., & Ashby, M. F. (1988). *Cellular solids: structure & properties*. Cambridge University Press. https://doi.org/10.1017/CBO9781139878326

Guillermic, R.-M., Franczyk, A. J., Kerhervé, S. O., House, J. D., Page, J. H., & Koksel, F. (2023). Characterization of the mechanical properties of high-moisture meat analogues using low-intensity ultrasound: Linking mechanical properties to textural and nutritional quality attributes. *Food Research International*, *173*, 113193. https://doi.org/10.1016/j.foodres.2023.113193

Högg, E., & Rauh, C. (2023). Towards a Better Understanding of Texturization during High-Moisture Extrusion (HME)—Part II: Characterization of Thermophysical Properties of High-Moisture Meat Analogues. *Foods*, *12*(12), 2283. https://doi.org/10.3390/foods12122283

Koksel, F., & Masatcioglu, M. T. (2018). Physical properties of puffed yellow pea snacks produced by nitrogen gas assisted extrusion cooking. *LWT*, *93*, 592–598. https://doi.org/10.1016/j.lwt.2018.04.011

Koksel, F., & Scanlon, M. G. G. (2012). Effects of composition on dough development and air entrainment in doughs made from gluten-starch blends. *Journal of Cereal Science*, *56*(2), 445–450. https://doi.org/10.1016/j.jcs.2012.05.013

Lee, J.-S., Kim, S., Jeong, Y. J., Choi, I., & Han, J. (2023). Impact of interactions between soy and pea proteins on quality characteristics of high-moisture meat analogues prepared via extrusion cooking process. *Food Hydrocolloids*, *139*, 108567. https://doi.org/10.1016/j.foodhyd.2023.108567

Luo, S., Chan, E., Masatcioglu, M. T., Erkinbaev, C., Paliwal, J., & Koksel, F. (2020). Effects of extrusion conditions and nitrogen injection on physical, mechanical, and microstructural properties of red lentil puffed snacks. *Food and Bioproducts Processing*, *121*, 143–153. https://doi.org/10.1016/J.FBP.2020.02.002

Marshall, M. R. (2010). Ash Analysis. In S. S. Nielsen (Ed.), *Food Analysis* (4th ed., pp. 105–115). Springer. https://doi.org/10.1007/978-1-4419-1478-1_7

Mateen, A., Mathpati, M., & Singh, G. (2023). A study on high moisture extrusion for making whole cut meat analogue: Characterization of system, process and product parameters. *Innovative Food Science & Emerging Technologies*, *85*, 103315. https://doi.org/10.1016/j.ifset.2023.103315

Mazlan, M. M., Talib, R. A., Chin, N. L., Shukri, R., Taip, F. S., Mohd Nor, M. Z., & Abdullah, N. (2020). Physical and Microstructure Properties of Oyster Mushroom-Soy Protein Meat Analog via Single-Screw Extrusion. *Foods*, *9*(8), 1023. https://doi.org/10.3390/foods9081023

Min, D. B., & Ellefson, W. C. (2010). Fat Analysis. In S. S. Nielsen (Ed.), *Food Analysis* (4th ed., pp. 117–132). Springer. https://doi.org/10.1007/978-1-4419-1478-1_8

Osen, R., Toelstede, S., Wild, F., Eisner, P., & Schweiggert-Weisz, U. (2014). High moisture extrusion cooking of pea protein isolates: Raw material characteristics, extruder responses, and texture properties. *Journal of Food Engineering*, *127*, 67–74. https://doi.org/10.1016/j.jfoodeng.2013.11.023

Pietsch, V. L., Bühler, J. M., Karbstein, H. P., & Emin, M. A. (2019). High moisture extrusion of soy protein concentrate: Influence of thermomechanical treatment on protein-protein interactions and rheological properties. *Journal of Food Engineering*, *251*, 11–18.

Scanlon, M. G., & Zghal, M. C. (2001). Bread properties and crumb structure. *Food Research International*, *34*(10), 841–864. https://doi.org/10.1016/S0963-9969(01)00109-0

Schreuders, F. K. G., Dekkers, B. L., Bodnár, I., Erni, P., Boom, R. M., & van der Goot, A. J. (2019). Comparing structuring potential of pea and soy protein with gluten for meat analogue preparation. *Journal of Food Engineering*, *261*, 32–39. https://doi.org/10.1016/j.jfoodeng.2019.04.022

Singh, R., & Koksel, F. (2021). Effects of particle size distribution and processing conditions on the techno-functional properties of extruded soybean meal. *LWT*, *152*, 112321. https://doi.org/10.1016/J.LWT.2021.112321

Sozer, N., Dogan, H., & Kokini, J. L. (2011). Textural Properties and Their Correlation to Cell Structure in Porous Food Materials. *Journal of Agricultural and Food Chemistry*, *59*(5), 1498–1507. https://doi.org/10.1021/jf103766x

Trater, A. M., Alavi, S., & Rizvi, S. S. H. (2005). Use of non-invasive X-ray microtomography for characterizing microstructure of extruded biopolymer foams. *Food Research International*, *38*(6), 709–719. https://doi.org/10.1016/j.foodres.2005.01.006

Wadell, H. (1935). Volume, shape, and roundness of quartz. *The Journal of Geology*, *43*(3), 250–280. https://www.jstor.org/stable/30056250

Wittek, P., Karbstein, H. P., & Emin, M. A. (2021). Blending Proteins in High Moisture Extrusion to Design Meat Analogues: Rheological Properties, Morphology Development and Product Properties. *Foods*, *10*(7), 1509. https://doi.org/10.3390/foods10071509

Wittek, P., Zeiler, N., Karbstein, H. P., & Emin, M. A. (2021). High Moisture Extrusion of Soy Protein: Investigations on the Formation of Anisotropic Product Structure. *Foods*, *10*(1), 102. https://doi.org/10.3390/foods10010102

Chapter IV: Conclusion and Future Work

The gas bubbles entrapped in the protein matrix changed the microstructure of the meat analogues. Bubbles of various sizes and shapes were visible in the reconstructed 2D images of meat analogues produced at 2.5 bar GP. Variations in the DT affected the maximum structure thickness, major diameter and sphericity of the bubbles. Moreover, the bubble's maximum structure thickness and sphericity were positively related to the DT, while the major median diameter was negatively associated. The microstructural changes brought by different DT-GP combinations led to the production of meat analogues with a wide variety of textural attributes. The variability in F_T (3.97-5.79 N), F_L (3.73-6.00 N), hardness (143.63-194.27 N), chewiness (106.01-150.49 N) and gumminess (115.15-161.85 N) demonstrated the potential of gas-assisted high-moisture extrusion cooking technique to improve and produce different types of meat analogues.

The texture profile of meat can vary significantly depending on the kind of meat product; for example, chicken and pork meat is comparatively softer than beef (Sun et al., 2023). It can be challenging to obtain meat analogues with a desired hardness using conventional high-moisture extrusion cooking without detrimental effects on other characteristics such as colour and degree of texturization. Gas-assisted high-moisture extrusion cooking, when optimized, has great potential in manipulating end-product texture without negatively impacting degree of protein texturization.

This study's scope was limited to using soy protein and nitrogen gas while altering only two extrusion operating parameters, i.e., DT and GP. All other extrusion operating parameters, such as dry feed rate, screw speed, barrel temperature profile and moisture content, were kept constant during gas-assisted high-moisture extrusion cooking. For the successful employment of

gas-assisted extrusion at the industrial level, it is crucial to check the feasibility of this novel extrusion process using other protein ingredients such as pea, wheat, oat, and canola proteins, as well as other blowing agents such as CO_2 and air at different injection pressures under a wide range of extrusion operating parameters. In addition to the experimental conditions studied, the current study only focused on the physical and microstructural characteristics of the meat analogues. However, future studies are required to understand the impact of gas injection on meat analogue's chemical and nutritional properties. Introducing gases like CO_2 that can solubilize in the melt and change the melt's pH (Masatcioglu et al., 2015) while gases like air can act as oxidizing agents (Sinaki et al., 2021, 2023) and therefore may affect protein size, structure, and protein-protein interactions in the meat analogues. Chemical and nutritional analyses including but not limited to SDS-PAGE, protein solubility, FT-IR spectroscopy, and protein digestibility are required to develop a holistic understanding of gas-assisted high-moisture extrusion technique.

References

Masatcioglu, T. M., Ng, P. K. W., & Koksel, H. (2015). Effects of formulation and extrusion cooking conditions on furfural and hydroxymethylfurfural content. *Journal of Cereal Science, 65*, 31–38. https://doi.org/10.1016/j.jcs.2015.06.003

Sinaki, N. Y., Paliwal, J., & Koksel, F. (2023). Enhancing the Techno-Functionality of Pea Flour by Air Injection-Assisted Extrusion at Different Temperatures and Flour Particle Sizes. *Foods, 12*(4), 889. https://doi.org/10.3390/foods12040889

Sinaki, N. Y., Tulbek, M., & Koksel, F. (2021). Oxidizing agent-assisted extrusion cooking of yellow peas and the techno-functionality of the resulting extrudate flours. *Journal of Food Processing and Preservation*, *45*(10). https://doi.org/10.1111/jfpp.15797

Sun, Y., Dong, M., Bai, J., Liu, X., Yang, X., & Duan, X. (2023). Preparation and properties of high-soluble wheat gluten protein-based meat analogues. *Journal of the Science of Food and Agriculture*. https://doi.org/10.1002/jsfa.12922

Appendices

Appendix 1: Effects of DT and GP on microstructure

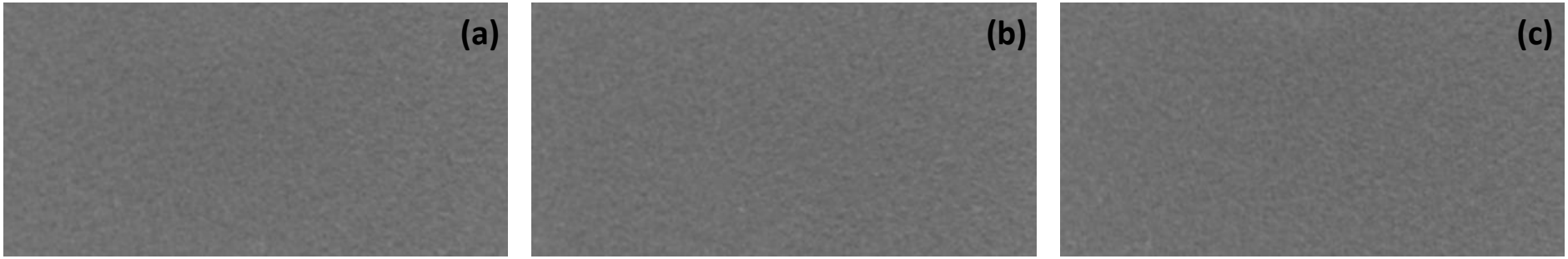

Figure A1.1: 2D reconstructed cross sectional slices of meat analogues produced at nitrogen gas injection pressure (GP) of 0 bar and long cooling die temperature (DT) of (a) 35 °C, (b) 50 °C and (c) 65 °C. The size of each slice is approximately 4 mm × 2 mm.

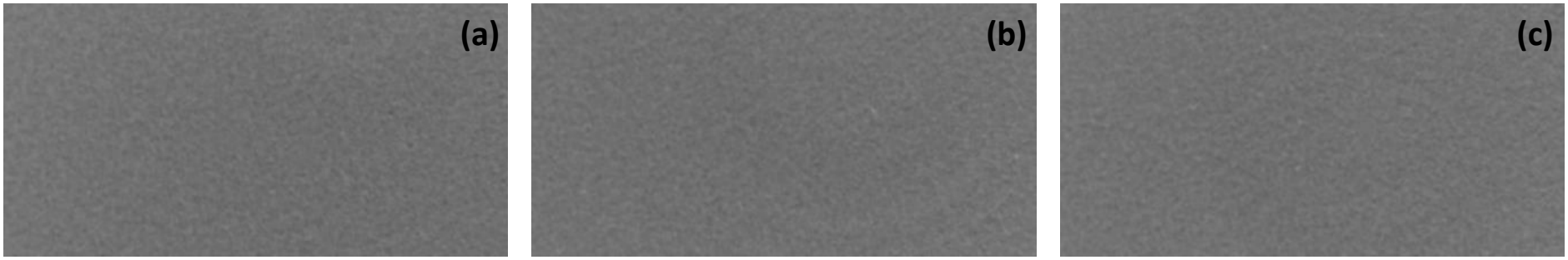

Figure A1.2: 2D reconstructed cross sectional slices of meat analogues produced at nitrogen gas injection pressure (GP) of 1 bar and long cooling die temperature (DT) of (a) 35 °C, (b) 50 °C and (c) 65 °C. The size of each slice is approximately 4 mm × 2 mm.